Study of the Global-scale Simulated Groundwater Recharge and Sensitivity Analysis of the VIC Model

Frontpage image: the global simulated groundwater recharge rates from the VIC model at the gridded scale, partial result from this study; the two water graphics are from free graphics of Canva.

Study of Global-scale Simulated Groundwater Recharge and Sensitivity Analysis of the VIC Model

Master Thesis – WSG 80436
Master program: International Land and Water Management
Chair Group: Water Systems and Global Change
Specialisation D: Flexible Configurations of Innovative Minds

Miranda Xiao
Register Number: 1195484
Supervisor: Dr. I.E.M. de Graaf
Examiners: Dr. I.E.M. de Graaf
Dr. S. Liu

March 20, 2024

Wageningen University,
Wageningen, the Netherlands

Acknowledgement

When I am writing this acknowledgement down, it reminds me of the reality of almost the end of my master's thesis, which is definitely a unique and unforgettable experience in my life.

I first want to express my deep gratitude to my supervisor, Dr. Inge de Graaf. This thesis cannot be accomplished without her meticulous guidance, mobilizing my enthusiasm to reflect on the topic from the literature I have read, broadening my perspective, encouraging me to independently explore and learn new concepts and scientific tools which foster a valuable learning process for me, providing assistance consistently during any stage of this thesis, guiding me through the analysis of the results, assisting me to have a comprehensive understanding of the topic, as well as providing constructive feedback and advice throughout the entire thesis. Besides, we managed to have one-hour meetings nearly every week, and I profoundly appreciate for those sessions beyond what words can express.

Meanwhile, I want to express my deep appreciation to Dr. Sida Liu, who helped run the global-scale hydrological models, explained the main concepts of the model simulations, helped me solve the technical problems I met, and provided useful tips and feedback during the completion of my thesis.

I am also truly thankful to my best friends (Shiya in China and Lavender in Canada). Although we are thousands of miles apart and even have various time differences, thank you all for being my side and giving me mental support all these years. Wish you all the best and luck in the future.

Last, but not least, here is my deepest appreciation to my beloved parents who support my dream, my life, and my everything unconditionally all the time. Thank you for not only being my parents but also my good friends. I love you.

Abstract

Groundwater recharge, as a critical factor in obtaining reliable estimations of groundwater availability, is still one of the least understood concepts in the groundwater system. Since limited observational datasets available at the global scale related to groundwater recharge, many well-known global-scale hydrological models tried to simulate the recharge to have a comprehensive understanding of the global groundwater system, but their results presented an underestimation by half (Berghuijs et al., 2022) when compared to the most updated observed recharge compilation by Moeck et al. (2020). To further analyse the reliability of the global-scale hydrological model in simulating groundwater recharge, this study focused on evaluating the simulated recharge from the Variable Infiltration Capacity (VIC) model which has experienced upgrades in its subsurface system coupled with the groundwater model of MODFLOW. This study thus evaluated the existing observed datasets from AQUASTAT (FAO, n.d.) and Moeck et al. (2020) and compared the observations to the simulated recharge from the VIC model at the country and gridded scales. Although the VIC model still presented an underestimation of groundwater recharge on a global scale, it demonstrated its improved estimations compared to other hydrological models, such as PCR-GLOBWB. Furthermore, this study applied several sensitivity tests to examine the corresponding changes in groundwater baseflows and depths when adjusting the recharge input, further inspecting the model sensitivity on the parameter of recharge. Based on the simulations, the baseflows displayed a tendency indicating that baseflow tends to escalate with increased recharge and decline with decreased recharge, particularly evident in humid regions. However, the simulated groundwater depths did not have a significant change when decreasing the recharge, while increasing the recharge resulted in unrealistic depths globally, highlighting the weakness of adjusting a single parameter in the simulation. Hence, it is important to consider adjusting multiple parameters and conducting additional sensitivity tests to further analyse the global-scale hydrological model sensitivity to changes in future studies.

Key words: VIC model, groundwater recharge, hydrological models, model sensitivity test, observed groundwater recharge

Table of Contents

List of Figures

List of Annex Figures

List of Tables

List of Annex Tables

List of Abbreviations

Abbreviations	Definitions
CRU TS	Climatic Research Unit Timeseries
CSV	Comma-separated value
DEM	Digital elevation model
ESPAM	East Snake Plain Aquifer Model
FAO	The Food and Agriculture Organization of the United Nations
GPCC	Global Precipitation Climatology Centre
GWIS	Global Water Information System
GWSWUSE	Groundwater-Surface Water Use
GW	Groundwater
LAI	Leaf area index
m	Meter
mm	Millimetre
MODFLOW	Modular Three-Dimensional Finite-Difference Flow Model
PCR-GLOBWB	PCRaster Global Water balance
RWR	Renewable water resources
the U.S.	The United States
VIC	Variable Infiltration Capacity
WGHM	WaterGAP Global Hydrology Model
WRI	World Resources Institute
yr	Year

Chapter 1. Introduction

Earth becomes a unique planet in the Solar System due to its 71% surface covered by liquid water (NASA, 2022; Williams, n.d.) that gave rise to life billions of years ago (NASA, 2022). However, the accessible freshwater resources for sustaining life remain very limited, constituting only 3% of the total water quantity globally, shown in Figure 1.1 (Cassardo & Jones, 2011; Musie & Gonfa, 2023). Unfortunately, nearly 70% of freshwater remains locked into glaciers and ice caps (Cassardo & Jones, 2011; Stephens et al., 2020), leaving easily accessible surface freshwater being profoundly restricted (Musie & Gonfa, 2023). In the meantime, global water demand keeps climbing (WWAP, 2018; Boretti & Rosa, 2019) owing to various factors including growing global population (U.N., n.d.) and intensive anthropogenic activities (Sidabutar et al., 2017; Thai-Hoang et al., 2022), while climate change adds more uncertainties to the water resources system (Nan et al., 2011; Kundzewicz et al., 2018). All the aforementioned aspects worsen the challenges we face in ensuring adequate and equitable water access and realizing sustainable water usage (Kummu et al., 2016; Boretti & Rosa, 2019; Reinecke et al., 2023). In such a difficult situation, groundwater has been raised more attention by researchers, driven by its high quality, abundant availability, relatively easy accessibility, as well as its frangibility (Ojo et al., 2012; Wardle, 2019).
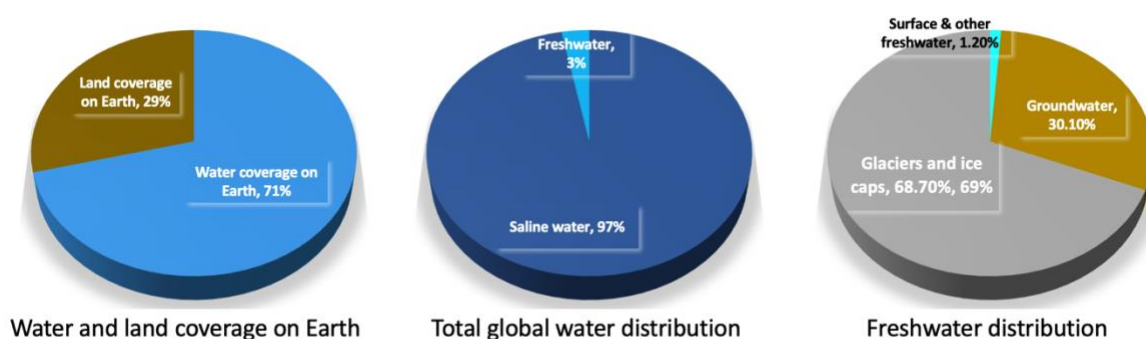
Figure 1.1. The total global water sources and freshwater distribution (USGS, 2019).

Groundwater has been extensively used by humankind for daily consumption, agricultural activities, and manufacturing since ancient times (Chilton, 1996; Government of Canada, 2013). Today, groundwater still holds a vital role in human life which supports as the primary drinking water source for more than two billion people (Grönwall & Danert, 2020) and carries about 70% agricultural activities (de Graaf et al., 2019). As an important part of the hydrological cycle, groundwater is also responsible for maintaining rivers, lakes, wetlands, and other related ecosystems (de Graaf et al., 2019). However, overexploitation, unsustainable management, climate change, and many other factors have caused groundwater levels to drastically drop in many regions in the past decades. Famiglietti (2014) presents that some major aquifers,

particularly those situated in arid and semi-arid regions, have experienced rapid declines in groundwater levels owing to overexploitation and a lack of effect management practice in the past decades. The immediate effects on these regions include the depleted wells, raised pumping costs for deeper boreholes, and lowered groundwater quality, and other unforeseen consequences are not limited to stream-flow depletion, sea-level rise, seawater intrusion, land subsidence, etc. (Famiglietti, 2014).

To enhance the sustainable management of groundwater resources and reduce further water level decline, we need to first have a comprehensive understanding of groundwater recharge process. Groundwater recharge is a critical factor in obtaining a reliable estimation of groundwater availability, assisting in determining the maximum groundwater abstraction from the aquifer to prevent the irreversible decline in groundwater levels and realize the sustainable usage of groundwater (Döll & Fiedler, 2007; Mohan et al., 2018; Berghuijs et al., 2022). However, groundwater recharge is also one of the least understood concepts in groundwater system, primarily owing to the least understanding of its rates (Moeck et al., 2020). Recharge rates become uncertain due to temporal and spatial variabilities (Moeck et al., 2020), resulting in sparse available data (Berghuijs et al., 2022). Many global-scale studies (e.g., de Graaf et al., 2015, 2017; Döll & Fiedler, 2007; Müller Schmied et al., 2021) used global-scale hydrological models to simulate groundwater recharge, while Moeck et al. (2020) doubt their reliability because many models still lack certain parameters due to the complexity of the properties and processes in the real groundwater system (Anderson et al., 2015), and lack the validation step of the simulations owing to the limited observational recharge data. Berghuijs et al. (2022) proved the concerns about the reliability of the simulations that many global-scale hydrological models (PCR-GLOBWB, WaterGAP) underestimated groundwater recharge by half compared to the observed dataset compiled by Moeck et al. (2020).

However, global-scale hydrological model approaches to simulate recharge are essential because complete in-situ recharge measurements are difficult to obtain worldwide (Moeck et al., 2020; Li et al., 2021). Accordingly, enhancing the existing global-scale models has become the foremost challenge to close the gap between simulated and observed groundwater recharge. The improvements of the models should aim to present a more accurate prediction of groundwater recharge at the global scale, bridging the measurement gap, and providing more compelling simulations for regional and continental usages (MacDonald et al., 2021). Moreover, the improved models can better integrate with the changing climate to present the impact of climate change on groundwater resource regionally and globally. With more accurate data available, researchers can better understand groundwater features and future potentials, proposing more feasible directions and suggestions, and guide policymakers to develop more sustainable policies for groundwater resource usage and management.

1.1.   Research Background

This section provides a comprehensive understanding of the research background from three perspectives. Section 1.1.1 gives insights into the groundwater recharge process, followed by the difficulty of its in-situ measurements. Then, section 1.1.2 describes the existing observed data from published paper and offer insights into some modelling approaches from other studies which focused on groundwater recharge at the global scale. Lastly, section 1.1.3 uncovers the initial motivation behind this study, deeply exploring into the findings that emerged from the original motivation.

1.1.1. Groundwater Recharge

Groundwater recharge process can be generalized as water moves downward by forces of gravity, crossing the water table, and forming an underground water reservoir (Balek, 1988; Anderson et al., 2015; Hartmann, 2022). Groundwater can be replenished naturally or artificially, as shown in Figure 1.2, but the artificial recharge approach will not be further explored in this paper because it is beyond the objectives, and this study will only concentrate on natural groundwater recharge. The water source of natural recharge mainly comes from precipitation, but it can also come from lakes, rivers, stream, and wetlands (Balek, 1988; Water Resources Mission Area, 2019). More in depth, natural recharge can be categorized as diffuse recharge and focused recharge mechanisms that groundwater system usually receives (Alley, 2009; Li et al., 2021; MacDonald et al., 2021). Diffuse recharge is the slow water movement from the land surface (precipitation and snowmelt) to the water table over large areas, infiltrating through the unsaturated zone (Alley, 2009; Li et al., 2021; MacDonald et al., 2021). Focused recharge refers to the non-uniform water movement from leaked surface water bodies, drainage through preferential flow paths, lateral flows from high mountains or rock fractures (Alley, 2009; Li et al., 2021; MacDonald et al., 2021). However, our study narrowed its focus on natural diffuse recharge, driven by the focused hydrological model we selected for analysis.
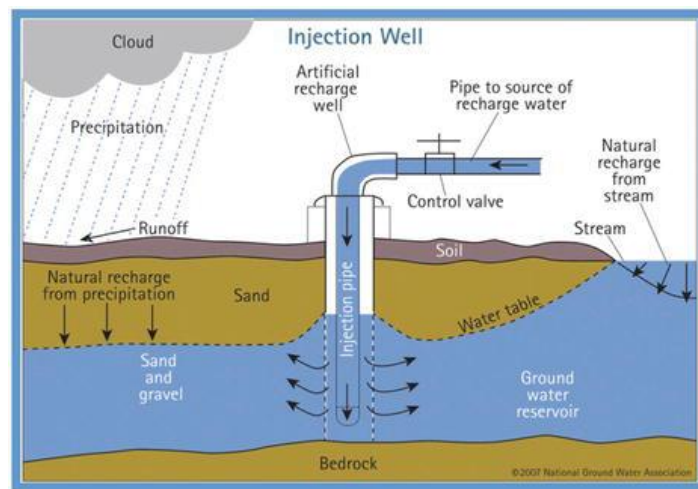
Figure 1.2. Groundwater recharge process, including natural groundwater recharge from precipitation and streams, and artificial groundwater recharge (Veeranna & Jeet, 2020).

As evident from the preceding description of the recharge process, groundwater originates from various sources, and the time and volume of each water source remain uncertain. Therefore, accurately determining groundwater recharge becomes a challenge, with many studies (e.g., Freyberg, 2015; Moeck et al., 2020) revealing the inherent difficulty in directly measuring groundwater recharge globally. Moeck et al. (2020) demonstrate that direct measurements of recharge are hard to obtain at the catchment scale, so experimental results can only come from the plot scale. Although the lysimeter is the common tool to measure the recharge directly at various sites globally without requiring regional considerations (Scanlon et al., 2002), expensive investment, high maintenance, restricted assessment, and other uncertainties broadly limit its usage (Moeck et al., 2020). Other methods also exist to quantify groundwater recharge based on different recharge processes and various climatic regions, including water-balance calculations, water-table fluctuations, environmental travers, etc. (Scanlon et al., 2002; Moeck et al., 2020; MacDonald et al., 2021). However, applying multiple techniques introduce bias at individual location (Moeck et al., 2020), reducing the reliability of the measurement when scaled up to a global scope. For example, water-balance calculation is more accurate in humid regions because humid regions usually have shallow water tables, and the recharge is mostly dominated by precipitation events in these areas, while recharge could accumulate more errors when applying this method to arid or semi-arid regions because small inaccuracies in other components can largely affect the accuracy of recharge rates (Scanlon et al., 2002).

Although there are numerous difficulties we face, it remains essential to understand groundwater recharge and strive for more accurate recharge rates because other crucial variables are also tightly connected to the recharge in the system. For example, some studies (Arnold et al., 2000; Schilling et al., 2021) used groundwater baseflow to estimate recharge with empirical approaches or hydrological models, indicating the interconnection between recharge and baseflow. Szilagyi et al. (2013) also analysed the relationship between the net groundwater recharge and depths in the shallow groundwater system when neglecting surface runoff. Therefore, understanding the responses from other variables to change in recharge pattern also helps us improve the hydrological models.

1.1.2. Available Groundwater Recharge Dataset: Observations vs. Simulations

Owing to the above-mentioned difficulties of obtaining the observed groundwater recharge, the complete observed dataset of recharge at the global scale is relatively rare. The Global Water Information System (GWIS) was established in 1993 to compile high-quality information on water resources and uses at a global scale (FAO, n.d.). AQUASTAT, as one of GWIS's complementary programs, was initiated to collect and publish the statistical information continuously on an annual basis (FAO, n.d.), which is the earliest, relatively complete groundwater recharge dataset at the global country scale to our knowledge. However, some studies (Döll & Fiedler, 2008; Mohan et al., 2018; Moeck et al., 2020) question its reliability as a standard comparison database, particularly on groundwater recharge.

Despite the challenges in collecting groundwater recharge data globally, there still exist datasets in small piles, but the information is more discrete until Moeck et al. (2020) published a compiled global dataset with groundwater recharge from 5237 locations worldwide by combining numerous datasets. However, the up-to-date dataset is still insufficient as a global database because more than half of the available data points are only present in the United States (U.S.), Australia, and Europe, while recharge data in Asia, Central Africa, and the Middle East are extremely limited. Additionally, Moeck et al. (2020) indicate that most recharge data are from the lower latitude regions, while recharge data from high latitudes and permafrost regions are limited because we still lack a comprehensive understanding of the recharge processes and rates in these areas.

With the challenges associated with acquiring complete global groundwater recharge dataset and the limited existing information, it is advisable to use global-scale hydrological models to upscale the regional data and fulfil the global dataset. Many studies (e.g., de Graaf et al., 2015; Döll & Fielder, 2008; Müller Schmied et al., 2021) have become the pioneers to upscale local findings on a broader scale.

In their pioneering work, Döll et al. (2002) first obtained the groundwater recharge estimation with WaterGAP Global Hydrology Model (WGHM), integrating data in the period of 1961-1990 at the global scale, revealing a consistent spatial distribution on groundwater recharge, precipitation, and runoff from the model simulation that high precipitation rate resulted in high recharge and high surface runoff rate resulted in low recharge. To validate the accuracy of the model, the researchers used the independent groundwater recharge estimations (WRI, 2000) as the observed dataset. Upon this comparison, the simulation displayed a tendency to overestimate the recharge in the territorial-large countries such as Brazil, Russia, and the U.S., except the countries with high recharge per unit area (such as New Zealand). Even though the average simulated recharge closely aligned with the independent estimations made by WRI (2000), shown in Table 1.1, the authors still question the reliability of the estimations owing to various uncertainties from the dataset. Several years later, Döll & Fielder (2008) used the upgraded version of WGHM (version 2.1) to simulate the global groundwater recharge for the same period (1961-1990) again. In this study, the authors used two precipitation datasets treated as equal reliability because of the uncertainty of the observed climate data at the global scale. The simulation results showed that differences between groundwater recharge got smaller within two precipitation datasets when the areal size increased. With the consideration of river discharge and improved spatial representation of total runoff, the authors still concluded that WGHM2.1 had overestimated the recharge by about 10-20% compared with the available observed data (FAO, 2005) at that moment.

Table 1.1. Average global groundwater recharge from various global-scale hydrological model simulations

Model name	Simulated by	Period	Average GW recharge (mm/year)	Validation	Conclusion
WaterGAP 2	Döll et al. (2002)	1961-1990	137 (Döll et al., 2002)	Yes, with WRI average values of 143 mm/year (2000)	The average recharge aligned with WRI value, but overestimated in territorial-large countries
WGHM 2.1	Döll & Fielder (2008)	1961-1990	107 (Berghuijs et al., 2022)	Yes, with L'vovich (1979) estimation, FAO dataset (2005)	Overestimated recharge by 10-20% if the observed dataset is trustable
PCR-GLOBWB	de Graaf et al. (2015)	1960-2010	111 (Berghuijs et al., 2022)	No	N.A.
WaterGAP 2.2d	Müller Schmied et al. (2021)	1981-2010	111 of diffuse recharge, 12.8 of focused recharge (Müller Schmied et al., 2021) 141(Berghuijs et al., 2022)	No	N.A.

As one of the global hydrological models, PCRaster Global Water balance (PCR-GLOBWB) is commonly used to estimate groundwater level, terrestrial water storage, and global water resources (van Beek & Bierkens, 2008; de Graaf et al., 2015, 2019). de Graaf et al. (2015, 2019) utilized the net groundwater recharge and surface water levels which were the outputs of PCR-GLOBWB model as the inputs to the Modular Three-Dimensional Finite-Difference Flow Model (MODFLOW) to simulate groundwater heads of an upper unconfined aquifer and estimate the spatial distribution of groundwater head variations. Within the PCR-GLOBWB model, the authors focused on steady-state groundwater recharge from 1960 to 2010, taking in charge with climatic, surface vegetative, edaphic, and topographical properties. According to the global map of groundwater recharge simulated by PCR-GLOBWB model, the largest recharge occurred in the Amazon basin, Southern Asia, coastal lines of Canada, part of the Netherlands, as well as Denmark with over 600 mm recharge per year. However, the results also showed that at least half of the world's territories only received recharge ranging from 0 to 25 mm per year.

Müller Schmied et al. (2021) present findings from their study by using WaterGAP model (version 2.2d), which is an updated version based on their published work in 2014, assessing global water resources. The model incorporates Groundwater-Surface Water Use (GWSWUSE) and the WGHM model, enabling the simulation of water withdrawals, streamflow, and terrestrial water storage anomaly, considering various water uses. As one of the WaterGAP model applications, the annual total renewable groundwater recharge (including both diffuse and focused recharge) showed that it accounted for 40% of the total renewable water resources from 1981 to 2010. The model also presented separate simulations for diffuse and focused recharges, where the global averaged diffuse recharge accounted for 111 mm/year, while the global averaged focused recharge was 12.8 mm/year. Notably, regions like the Amazon basin, Central Africa, and Southern Asia received over 300 mm diffuse recharge annually, while Northern Africa, Central Asia, and parts of Western Asia received less than 2 mm diffuse recharge. In terms of focused recharge, the simulation

showed that most regions received less than 2 mm recharge per year worldwide. Despite a lack of validation with the observed data, this study still provides valuable insights into global groundwater patterns with diffuse and focused recharge (Müller Schmied et al., 2021).

According to the summarization of the simulated average recharge on a global scale from Table 1.1, we can observe a minimal difference between WGHM2.1 (Döll & Fielder, 2008), PCR-GLOBWB (de Graaf et al., 2015), and WaterGAP 2.2d (Müller Schmied et al., 2021). However, we need to notice that the sources of the value of the global average recharge were inconsistent, as some authors calculated the average recharge values, while others were only found from the paper of Berghuijs et al. (2022). Although the displayed differences are minimal in the simulated global average recharge, disparities still exist during the simulation processes in different models. For example, Döll & Fielder (2008) used the two historical precipitation datasets from the Global Precipitation Climatology Centre (GPCC) and Climatic Research Unit Timeseries (CRU TS 2.0), while de Graaf et al. (2015) applied climate data from CRU TS 2.1. de Graaf et al. (2015) considered the interactions with surface water bodies, while Döll & Fielder (2008) did not take into account these interactions. However, these simulated groundwater recharge from various models still shared a similar trend in the spatial distribution globally that some areas in humid regions received the highest recharge rates such as the Amazon Basin, Central Arica, and Southern Asia. In contrast, arid and semi-arid regions had the lowest recharge rates, particularly in the Sahara region, the Middle East, and Central Asia (Döll & Fielder, 2008; de Graaf et al., 2015; Müller Schmied et al., 2021).

1.1.3. Analysis of the motivated paper of this study

As aforementioned, some studies (e.g., Döll et al., 2008) have concluded that the hydrological models overestimate the groundwater recharge at the global scale. However, Berghuijs et al. (2022) contradict the statement of overestimation and proposed that the well-known hydrological models, such as PCR-GLOBWB and WaterGAP, underestimated the recharge on average by half when compared with the observed dataset, synthesized by Moeck et al. (2020), presented in Figure 1.3. Hartmann et al. (2017) proposed the possibility of these underestimations of groundwater recharge due to the ignorance of subsurface heterogeneity in these hydrological models according to their regional analysis across rock landscapes (Berghuijs et al., 2022). Some studies (e.g., Cuthbert et al., 2019) also
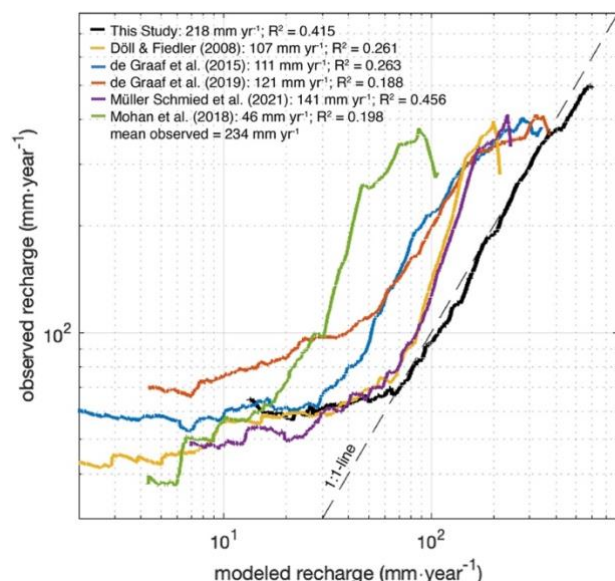
Figure 1. 3. Comparison of observed data with various global-scale hydrological model simulations (Berghuijs et al., 2022).

believed that these hydrological models showed an exaggerated sensitivity of recharge to climate change, particularly in the arid regions (Berghuijs et al., 2022). However, how widespread of the bias between the observation and simulation on groundwater recharge still remains unclear.

Different from the previous studies which used the global-scale hydrological models to simulate groundwater recharge, Berghuijs et al. (2022) used the mathematical formulas that target on climate aridity to compute the recharge and validated with the recent observed dataset compiled by Moeck et al. (2020). The findings demonstrated a significant impact of climate aridity on recharge fractions globally, presenting that the recharge fraction decreased with increasing aridity, except in the permafrost and extremely humid regions. The average groundwater recharge is 218 mm/year with aridity parametrization from the calculations by Berghuijs et al. (2022), closing to the observed mean recharge (234 mm/year) obtained by Moeck et al. (2020). However, the annual average recharges from the global-scale hydrological models were far away from the observed value, underestimating the annual recharge roughly by half (Figure 1.3, Table 1.2). Although Berghuijs et al. (2022) showed a closer average groundwater recharge estimation, we still cannot neglect the weaknesses of this approach. As the authors acknowledged themselves, there are other factors such as surface runoff that can greatly impact on groundwater recharge, but these factors were ignored in the mathematical approach. Besides, we also noticed when Berghuijs et al. (2022) compared the simulated average recharge from the machine learning approach (Mohan et al., 2018) to the observed average recharge, the relative difference reached up to 80%. However, this comparison is less convincing at the global scale when regarding the approach of Mohan et al. (2018) as a distant underestimation of groundwater recharge because Berghuijs et al. (2022) only considered 14% of the total available observations (715 sites out of 5237 sites). In the meantime, we should not ignore that most of the observed data primarily encompasses the regions in Australia, the U.S., and Europe, so the limited coverage is particularly remarkable when considering the global scale.

Table 1.2 . Simulated global average groundwater recharge from various methods (Berghuijs et al., 2022)

Model name	Published by	Period	Average GW recharge (mm/year) from Berghuijs et al. (2022)	Validation	Validated results
WGHM 2.1	Döll & Fielder (2008)	1961-1990	107		Underestimate by 54%
PCR-GLOBWB	de Graaf et al. (2015)	1957-2002	111	The simulated average groundwater recharge from each approach was validated with the observed average recharge of 234mm/year (Moeck et al., 2020),	Underestimate by 53%
Machine learning	Mohan et al. (2018)	1981-2014	46		Underestimate by 80%
PCR-GLOBWB	de Graaf et al. (2019)	1960-2100	121		Underestimate by 48%
WaterGAP 2.2d	Müller Schmied et al. (2021)	1901-2016	141		Underestimate by 40%
Empirical formula	Berghuijs et al. (2022)	N.A.	218		Underestimate by 7%

1.2.   Research Objectives and Research Questions

The motivation for this study was initiated from the paper of Berghuijs et al. (2022) in which the authors present all global-scale hydrological models underestimated groundwater recharge at least by half. Therefore, we want to deeply explore the existing observed groundwater recharge datasets, and compared to the historical data of the simulated groundwater recharge from other global-scale hydrological models aside from the mentioned models by Berghuijs et al. (2022), further investigating the reliability of the global-scale model. We want to understand the sensitivity of the global-scale hydrological models to changes and the impacts on the groundwater system when changing the groundwater recharge. We thus can discover the errors and/or missed processes during the simulation and provide sufficient recommendations for further research.

To fulfil the objectives of this study, the main research question is formulated with the following subsequent research questions:

What is the reliability of the simulated groundwater recharge data at the global scale, and what are the impacts of the uncertainty in recharge on the groundwater system?

① What are the characteristics of the existing observed recharge datasets? What are the methodologies applied to each observational dataset?

② What are the performances of other global-scale hydrological models in modelling groundwater recharge compared to each observational recharge dataset?

③ What are the impacts on the groundwater system when we modify groundwater recharge in the simulation?

④ What are the errors or processes we missed potentially in the simulation that contribute to the disparities between the observed and simulated groundwater recharge at the global scale?

Chapter 2. Methodology

This chapter describes the applications and detailed steps that we implemented during this study. Meanwhile, this chapter explains the reasons behind every key material and method we chose in the study to provide a comprehensive understanding of the objectives and a closer insight into the research questions before exploring the results of this study.

2.1.　Focused hydrological models in this study

We have introduced a few well-known global scale hydrological models in the previous chapter (section1.1.2), including WGHM, PCR-GLOBWB, and WaterGAP, and provided concise explanations regarding the groundwater recharge simulation outcomes for each model (Döll & Fielder, 2008; de Graaf et al., 2015; Müller Schmied et al., 2021). In this study, we chose to concentrate on the evaluations of the simulated recharge and sensitivity of the Variable Infiltration Capacity (VIC) model, a widely used global-scale hydrological model in numerous applications of water and energy balances (Liang et al., 1994; Hamman et al., 2018).

The VIC model was initially introduced by Wood et al. (1992), integrated with general circulation model (GCM) within gridded cells to depict spatial variations in infiltration capacity and to tackle the unsolved challenge of determining the appropriate level of complexity for accurately representing spatial heterogeneity in land-surface parametrization. Liang et al. (1994) published the implemented version of VIC with both surface energy and water balance. In this updated model, each gridded cell consists of three general layers (Figure 2.1), the canopy, the upper soil, and the bottom soil layer, concerning both surface and subsurface systems. The canopy layer represents the condition of the surface land, detailed into various land cover types which are determined by the leaf area index (LAI), canopy resistance, and fraction of roots in the soil layers. When the surface is only covered by bare soil class, the model then regards no canopy layer in the simulation. The upper and bottom soil layers together form the soil column in the model. The upper soil layer represents the dynamic response of the soil column to precipitation, while the bottom soil layer describes the slow changes in soil moisture between storms and it only responds to precipitation when the upper layer is saturated (Liang et al., 1994).
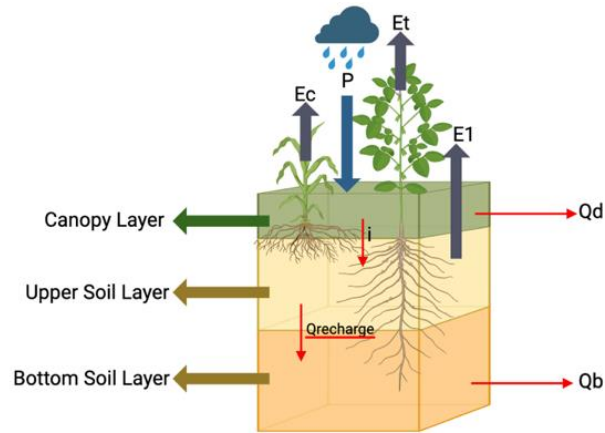
Figure 2.1. Schematic concept of water-flowing processes in one gridded cell in the VIC model (Liang et al., 1994).

According to the law of conservation of mass, the water balance of the hydrologic system can be generalized as the inflow equals the sum of the outflow and change in storage. In the VIC model, the inflow only considers from atmosphere (VIC Model, 2021), mainly precipitation (P), while the outflow includes evapotranspiration, surface runoff, and subsurface runoff. The total evapotranspiration of one gridded cell considers three aspects: evaporation from every vegetation class (E_c) at the canopy layer, transpiration from every vegetation class (E_t), and evaporation from bare soil with only the considerations of the upper soil layer (E_1), as shown in Figure 2.1. When there is a rainfall event, the canopy layer receives an amount of water for vegetation taken up, while a part of rainwater continuously moves from the canopy layer into the soil layer, referring to the infiltration process (i) (Mahapatra et al., 2020). However, when there is excessive rainwater that exceeds the maximum capacity of the soil on the surface land, this amount of rainwater will leave the gridded cells as surface runoff (Q_d) before entering the upper soil layer. In the VIC model, soil moisture content is a significant factor which depends on the maximum infiltration capacity and infiltration shape parameter in calculating water balance because it affects surface runoff and the drainage water from the upper layer ($Q_{recharge}$). When the upper layer is saturated, the model assumes water then moves only to the bottom layer driven by gravity, named as $Q_{recharge}$. Correspondingly, subsurface discharge (Q_b) only considers the excess water from the bottom soil layer (Liang et al., 1994).

Although the VIC model has been intensively implemented into various studies of streamflow, evapotranspiration, soil moisture, and water resources (Wang et al., 2017; Guo et al., 2020; Dash et al., 2021), fewer studies related to the groundwater system due to the limited insights into groundwater dynamics with the current version, even the model has been continuously upgraded by researchers (Liang et al., 2003; Sridhar et al., 2017; Hamman et al., 2018; Droppers et al., 2020). In upgrading the VIC model, many researchers (e.g., Sridhar et al., 2017) chose to couple with the widely used groundwater model, MODFLOW. MODFLOW is a three-dimensional model that is widely used in groundwater simulations

(Loudyi et al., 2014), considering the physical parameter and boundary conditions to simulate the steady and unsteady groundwater flow through a porous medium in unconfined and confined aquifers with a finite-difference method (Loudyi et al., 2014; Sridhar et al., 2017; Zeydalinejad, 2022).

At present, the research group at Wageningen University is improving the subsurface system of the VIC model (VIC-WUR) by integrating with MODFLOW, with the aim of scaling up to a global scale. The VIC-WUR model consists of four layers. The developers keep the canopy and upper soil layers from the original model but use the unconfined and confined layers to replace the bottom soil layer (Figure 2.3) to enhance the simulation of subsurface hydrological dynamics in order to have a comprehensive understanding of the global groundwater system. The MODFLOW model is used to simulate groundwater in the unconfined and confined aquifers, assuming, in this study, steady-state natural conditions with editable boundary conditions. In the VIC-WUR model, water continuously moves downward from the upper soil layer to the unconfined layer due to the force of gravity ($Q_{recharge}$ in Figure 2.3), mirroring the behaviour of the VIC model published by Liang et al. (1994). $Q_{recharge}$ also serves as the input parameter for MODFLOW, facilitating the calculations of groundwater heads and baseflows between surface and groundwater.
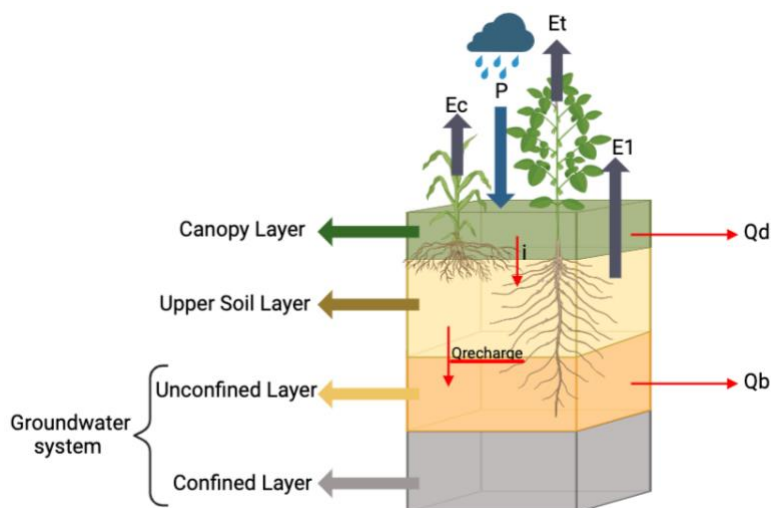
Figure 2.2. Schematic concept of water-flowing processes in one gridded cell in the VIC-WUR model.

Hence, this study focuses on evaluating the groundwater recharge simulation from the VIC model and the sensitivity tests of the simulated groundwater baseflows and depths when adjusting the recharge input to contribute to the model development. Besides the analysis of the VIC simulations, this study also used simulated groundwater recharge from the PCR-GLOBWB model to compare the relative accuracy and reliability of the recharge obtained from the VIC model. Since the PCR-GLOBWB model is not the focused model primarily in this study, no further explorations of its properties and mechanism will be provided in this study.

2.2. Exploration of the existing observed datasets

As aforementioned difficulties of acquiring a complete observed groundwater recharge dataset globally (section 1.1.2), the AQUASTAT dataset (FAO, n.d.) and Moeck dataset (Moeck et al., 2020) are relatively comprehensive observed datasets available on a global scale to our knowledge. Therefore, we are going to further explore the performances of these two observed datasets.

2.2.1. The AQUASTAT dataset

According to the information from the online database, the global groundwater recharge data from AQUASTAT[1] is only available at the country scale annually. Since the VIC model regards the period of 1970-2000 (31-year) as the historical data, we also gathered the observed groundwater recharge data globally at the country scale from AQUASTAT in the 31-year period to keep the consistency.

The AQUASTAT dissemination system uses the term 'total renewable groundwater' which we regarded as groundwater recharge in this study since the official definition of total renewable groundwater is "the sum of the total internal and external renewable groundwater resources" (FAO, 2019).

We used the programming language R to average the annual groundwater recharge for each country over the 31-year period. We converted the units of groundwater recharge rate to mm/year (Eq. 1) for a common expression since AQUASTAT uses the volumetric units ($m^3/year$), and we acquired the territorial area of every country from Quantum Geographic Information System (QGIS). We used RStudio to visualize the country-scale recharge rates worldwide.

$$GW\ recharge\ (mm/year)\ =\ \frac{Country's\ GW\ recharge\ (m^3/year)}{Area\ of\ country\ territory\ (m^2)}*1000 \qquad \text{Eq.1}$$

2.2.2. The Moeck dataset

The Moeck dataset, compiled from 56 studies by Moeck et al. (2020), consists of 5237 plot-scale locations globally. However, more than half of the data is located in Europe, the U.S., and coastal areas of Australia. Given the constrains of available data and the inability to upscale, we chose to directly extract the original point data and map from Moeck et al. (2020) for analysis at this stage.

In addition, we further explored the methodologies that AQUASTAT and Moeck datasets applied to have a comprehensive understanding and facilitate thorough analysis of these observed datasets.

2.3. Groundwater recharge from the VIC model

To evaluate the simulated groundwater recharge from the VIC model, we chose to examine the similarities and differences between the simulated and observed recharge rates.

---

[1] The historical data for groundwater recharge from AQUASTAT is available from 1966 to 2018 at the country scale annually (FAO, n.d.).

We received the rasterized monthly historical groundwater recharge globally from the VIC-WUR model from 1970 to 2000, with a resolution of a half degree (30-arcmin) in a file of Network Common Data Form (NetCDF). We used R to process the simulated groundwater recharge. We first organized the time units to have monthly recharge data because the time unites presented as days from 0001-01-01 00:00:00 in the file (see Annex 1, Figures A1.1, A1.2). Then, we reshaped the rasterized data to vector data with coordinates and calculated the average recharge for each year in the 31-year period (see Annex 1, Figure A1.3), and followed by a calculation of the average groundwater recharge over the 31 years at each presented coordinate (see Annex 1, Figures A1.4).

2.3.1.   the VIC data vs. the AQUASTAT data

To keep the consistency and be comparable with AQUASTAT which only has data at the country scale, we converted the VIC recharge again to match the country-scale format using QGIS. This involved creating a layer of the world map as a reference and importing the VIC data as another layer, the utilizing the 'Join Attributes by Location' tool to create a new vector layer align the VIC recharge with the world map layer. We recreated a vector layer of the VIC recharge because the VIC recharge was saved in a comma-separated value (CSV) file exported from R. Next, we exported the new vector layer and imported it into R to compute the average recharge for each country, considering that a single country encompasses multiple coordinates. We thus had the averaged simulated groundwater recharge at the country scale. The following step was to visualize the VIC country-scale recharge on a global map in QGIS, conducting a comparative analysis with the observed AQUASTAT map. Lastly, we used R again to generate a scatter plot between the VIC and AQUSTAT recharge rates at the country scale to evaluate if the simulated recharge rates were underestimated, overestimated, or aligned with the observed recharge rates.

2.3.2.   the VIC data vs. the Moeck data

We chose to use both vector and rasterized data through QGIS and R for mapping and comparing the VIC and Moeck datasets to different extents due to the nature of the Moeck dataset, which consists of point data only. This integrated approach provides a holistic perspective for processing and analysing the results.

We initiated the process in QGIS by establishing a world map layer for reference. Then, we converted the point data from Moeck's dataset into vector data, also facilitating in the following rasterization. This conversion involved generating a rectangle polygon grid layer with an extent of longitude ranging from -180° to 180° and latitude ranging from -90° to 90°. Next, importing the Moeck point data as a new layer, and employed the 'Join Attributes by Location' tool with the grid layer to obtain a new vector layer for the Moeck data. We exported the Moeck vector layer and calculated the average recharge in each gridded cell in R since some cells contained multiple data points (Figure 2.4), ensuring each gridded cell only contained one recharge value.
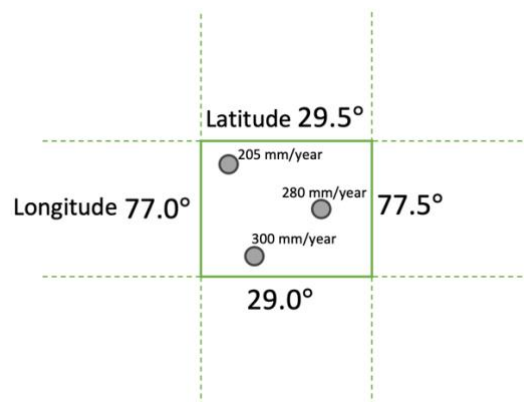
Figure 2.3. Concept of multiple recharge data points in the Moeck data located in one gridded cell.

The VIC vector data was processed in QGIS following a similar procedure as the Moeck data because the VIC recharge was saved in a CSV file. However, it is unnecessary to calculate the averaged recharge in each cell of the VIC recharge because every gridded cell only contained one recharge value.

With the establishments of the Moeck and VIC layers, we used the 'Join Attributes by Location' tool again to merge the two datasets, creating a new layer with coordinated Moeck and VIC recharge rates. The latest layer was exported and imported into R for a scatter plot to analyse the distance between the simulated and observed datasets.

In addition, we enhanced our approach by rasterizing the VIC and Moeck vector layers separately with the 'Rasterize (vector to raster)' tool in QGIS, resulting in the visualized map with colour gradient and enriching the analytical perspectives.

2.3.3. the VIC data vs. the PCR-GLOBWB data

We received the averaged groundwater recharge from the PCR-GLOBWB model in the rasterized format with a resolution of 5arcmin globally. Therefore, we first needed to adjust the resolution of the PCR-GLOBWB recharge to match of the VIC recharge by converting it to a half degree (30-arcmin) in QGIS. We began to import the PCR-GLOBWB data into QGIS, promptly exporting it again in order to adjust the resolution to 30-arcmin within the saving window, resulting in creating a new raster layer with resolution of a half degree. Them, we used the 'Raster pixels to points' tool to convert the new raster layer to a point-data layer, followed by using the 'Join Attributes by Location' tool with the grid layer to acquire a vector data layer. We saved the attributes of this vector layer in a CSV file and imported into R to merge with the VIC vector data, which we obtained in section 2.3.2 and illustrated a scatter plot.

2.4. Model Sensitivity tests

Following the findings of Berghuijs et al. (2022) that the well-known global-scale hydrological models have significantly underestimated groundwater recharge, our study also aims to explore the potential

impacts on the groundwater system when halving and doubling the recharge. An integration between the VIC and MODFLOW models occur since the output from the VIC model (groundwater recharge) would be the input for the MODFLOW to simulate groundwater heads and baseflow. The simulated groundwater depths would be evaluated correspondingly, conveying the same concept as the simulated groundwater heads from different perspectives (Figure 2.5), with a more straightforward interpretation.
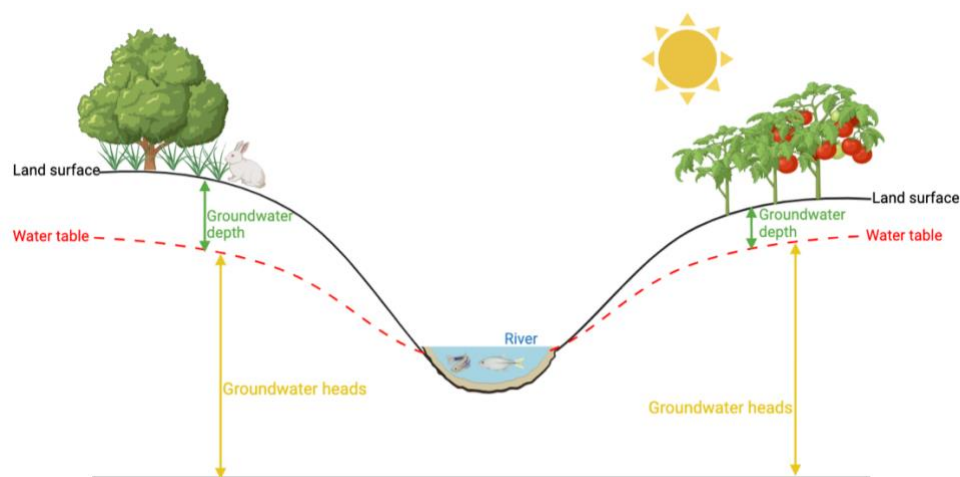
Figure 2.4. Cross-sectional diagram of the relationship between groundwater heads and groundwater depth.

However, the MODFLOW model operates with a resolution of 5-arcmin, while the VIC model has the resolution of 30-armin (half degree). We firstly adjusted the resolution of the VIC recharge from 30- to 5-arcmin using QGIS. We re-used the rasterized VIC recharge from section 2.3.2 and specified the resolution of 5-armin in the 'Wrap (Reprojection)' tool in QGIS for conversion, resulting in a new raster layer of VIC recharge with a resolution of 5armin.

To create a baseline comparison, we used the original recharge from the VIC model, named 'recharge factor 1,' as the input for MODFLOW to simulate groundwater heads (named 'GW factor 1') and baseflow (named 'baseflow factor 1). To calculate groundwater depth (named 'GWD factor 1'), we imported simulated groundwater heads of the top layer and the digital elevation model (DEM) into QGIS using the 'Raster Calculator' tool with Eq. 2:

$$Groundwater\ depth = DEM - Groundwater\ heads \qquad \text{Eq. 2}$$

As aforementioned, we want to analyse the impacts on the groundwater system with adjusted recharge. To obtain different recharge values, we used the 'Raster Calculator' tool to halve and double the original recharge in QGIS, receiving two rasterized layers (named 'recharge factor half' and 'recharge factor 2'). Subsequently, we exported the adjusted recharge layers as raster files from QGIS and applied them as input in the MODFLOW model to simulate groundwater heads and baseflow respectively. We followed the same procedure from 'GWD factor 1' to calculate groundwater depth for the halved and doubled recharge.

To have a thorough analysis of the changes in the groundwater system, we used the 'Raster Calculator' tool in QGIS to calculate absolute (Eq. 3) and relative differences (Eq. 4) of the simulated groundwater heads, groundwater depths, and groundwater baseflow from 'recharge factor 1', 'recharge factor half', and 'recharge factor 2,' respectively.

$$Absolute\ differnce = abs(Baseflow_{factor\ 2}) - abs(Baseflow_{factor\ 1}) \qquad \text{Eq. 3}$$

$$Relative\ difference = \frac{abs(Baseflow_{factor\ 2}) - abs(Baseflow_{factor\ 1})}{abs(Baseflow_{factor\ 1})} * 100\% \qquad \text{Eq. 4}$$

Chapter 3. Results

This chapter presents the direct outcomes derived from the methodologies outlined in Chapter 2. Each subsection targets the results pertinent to the corresponding research question, following the sequential order, presented in section 1.2.

3.1.   Exploration of the existing observed datasets

This section describes the AQUASTAT and Moeck observed datasets, with detailed depictions of the resulting figures and methodologies applied in each dataset.

3.1.1.   the AQUASTAT dataset

Although AQUASTAT presents the information of water resources of 191 countries, 169 countries had available information on groundwater recharge, so we only considered these countries in the analysis spanning from 1970 to 2000. Figure 3.1 depicts the groundwater recharge rates at the country scale in a world map. The complete table of recharge rates for each country can be found in Annex 2, table A2.1.
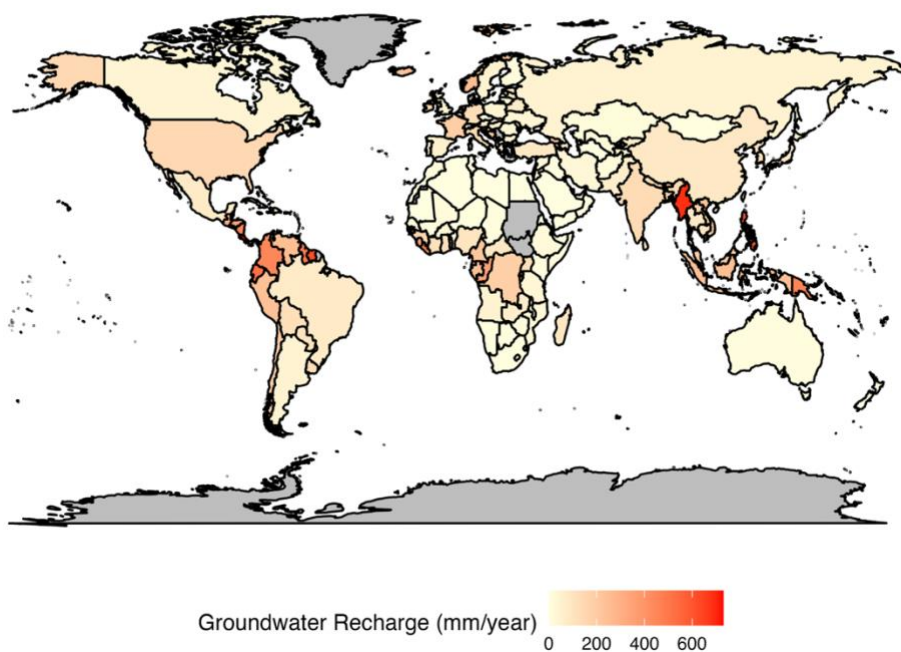
Figure 3.1. Map of the observed groundwater recharge rates at the country sale based on the AQUASTAT records.

Upon inspecting the map results depicted in Figure 3.1, the conspicuous observation is the presence of grey-shaded regions, indicating a lack of available recharge data in these areas. Antarctica, Greenland, Sudan, and South Sudan are prominent owing to their large territorial land area in Figure 3.1. There are also a few countries without available recharge information, but they are difficult to observe on the map owing to their small territorial land areas.

Costa Rica in Central America has the highest average groundwater recharge rate of 730.1 mm/year, while Mauritania in Africa holds the lowest recharge rate with 0.29 mm/year. The global average groundwater recharge rate is 145.57 mm/year over the 31-year period. Out of the total 169 regions, 55 (about 33%) regions had recharge rates above the global average. Conversely, more than half of the regions fell below this global average, contributing a significant presence of light-yellow colour shading in Figure 3.1. For example, most of the regions present a light-yellow colour in Africa, while a few countries are shaded in light orange near Central Africa. Myanmar presents a notable red shade in Asia with an average recharge rate of 684.45 mm/year, as the second-highest rate globally. The island countries in South Asia show relatively high recharge rates with orange-to-red shades on the map. However, the average recharge rates tended to drastically diminish as we move towards the northern and central regions of Asia, such as Kazakhstan (12.47 mm/year), Mongolia (3.9 mm/year), and Turkmenistan (0.86 mm/year). In Europe, we notice that France, Germany, Italy, Iceland, and Norway are shaded in a notable light orange colour, but regions in Eastern Europe had a tendency of lower recharge rates. The three predominant countries in North America had a distinct recharge rate: the U.S. had the highest rate of 146.12 mm/year, followed by Mexico with a recharge of 76.58 mm/year, but Canada only had an average rate of 37.22 mm/year. The countries in Central America and northern regions in South America showed relatively high recharge rates, while the recharge rates slightly declined towards the southern regions of South America.

3.1.1.1.   Methodologies applied by AQUASTAT

AQUASTAT defined the renewable water resources a "the long-term average annual flow of rivers (surface water) and recharge of aquifers (groundwater) generated from precipitation" (FAO, 2019). This definition is further divided into natural and actual renewable water resources (RWR) by AQUASTAT. Natural RWR considers both internal and external water resources on surface water and groundwater, while actual RWR is varied by time and consumption, requiring to a specific year (FAO, 2003). The internal RWR represents the volume of water generated within a country, whereas the external RWR denotes the quantity of water generated in upstream countries. The evaluation of a country's RWR was initially outlined by AQUASTAT in 1996, using the water resource accounting approach. The total RWR of a country involves both natural RWR internally and externally, and actual RWR components, and the detailed relationships between each RWR described in Annex 2, Figure A2.1. However, this study primarily focuses on groundwater, so the detailed information regarding surface RWR will not be explicitly discussed in this paper (FAO, 2003).

In general, there are six steps involved in computing RWR by country (Annex 2, Figure A2.2). The initial step entailed selecting the most accurate data sources for subsequent calculations. Although there were multiple sources, AQUASTAT prioritized national sources and literature over others. Consequently, the quality of results was related closely to national data production and reporting system. Additionally, a significant part of the data was obtained from country surveys conducted by the AQUASTAT programme

across 150 countries from 1993 to 2000. These data were thoroughly evaluated by experts to ensure their reliability before further calculations. In the countries with limited information on water resources or unreliable national data, AQUASTAT used estimated values derived from model simulations and satellite imagery. With the available data source, AQUASTAT assessed the internal RWR, the natural and actual external RWR, and the total RWR. Furthermore, the AQUASTAT programme also calculated the dependency ratio in annual averages to examine a country's dependency on external water sources. Lastly, the inflows and outflows were cross-checked between countries to ensure the consistency of the results (FAO, 2003).

3.1.2.   the Moeck dataset

There are 5237 observational points of groundwater recharge rate across the globe according to the compile dataset by Moeck et al. (2020), shown in Figure 3.2, spanning from 0 to 1945.51 mm/year, with an average rate of 234 mm/year. However, the data distribution was extremely uneven, with more than half of the observational points concentrated on Europe, the U.S., Southern Africa, and the coastal regions of Australia. Extremely limited data are available in South America, the Middle East, and Asia. In contrast, there is no single data available in North and Central Asia, island countries in South Asia, Central America, Arctic, and Greenland.
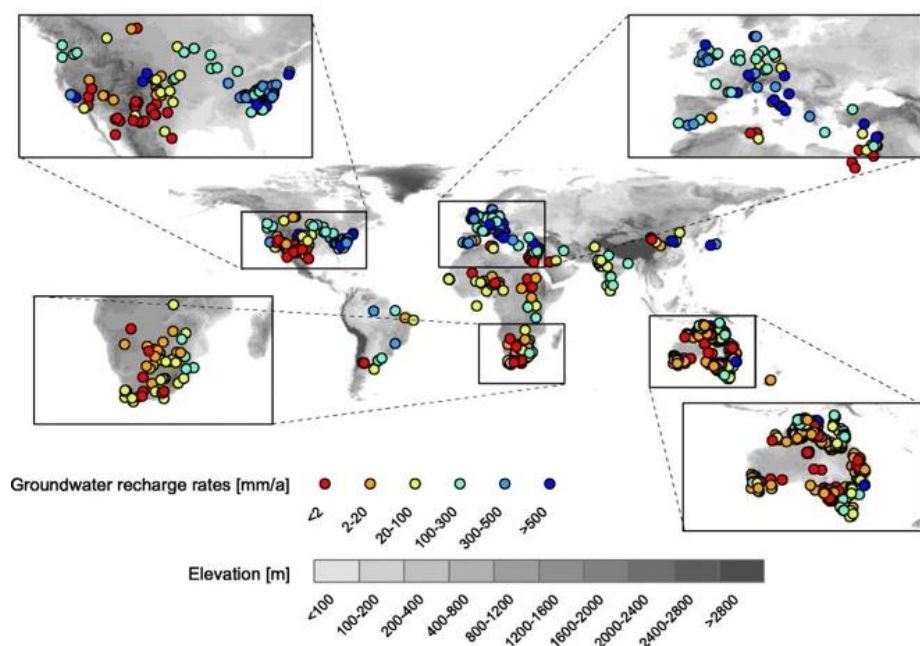
Figure 3. 2 Locations of global groundwater recharge data availability (Moeck et al., 2020).

As one of the highlighted areas, recharge rates in Europe displayed a relatively high value ranging from light blue to dark blue colour, indicating that most of the recharge rates surpassed 100 mm/year, and representing a sub-humid condition. Notably, Italy and its surrounding regions stand out owing to their

substantial recharge rates, which exceeded 500 mm/year. According to the data in the U.S., we can discover that the eastern region generally presented high recharge rates, of over 100 mm/year. In contrast, the regions in the Great Plains and Midwest tended to have lower recharge rates, with the majority of data points falling below 100 mm/year. The northeast high-elevation areas where most points were shaded in red, had an annual recharge of less than 2 mm, recognized as hyper-arid regions. In Southern Africa, most of the recharge rates were distributed between 2 and 100 mm/year, describing an arid to semi-arid condition. There are a few points that exceed 100 mm/year, but they are concentrated in the eastern regions. Several points displayed a recharge rate of less than 2 mm/year as a hyper-arid condition, spreading from the middle to further southern regions. In Oceania, almost all available data were located in Australia, especially along the coastal regions which displayed a tendency for high recharge rates, while the rate decreased toward Central Australia. Despite this trend, only a few points along the coastal regions were shaded in light and dark blues, which represent the high recharge rate.

The scarcity of available data in South America and the Middle East hinders a comprehensive exploration of the spatial distribution of groundwater recharge rates in these regions. Even within Asia, the available data was primarily concentrated in India. In India, recharge rates generally ranged from 20 to 300 mm/year. However, it is still difficult to recognize any clear tendencies in recharge rates in China and Japan owing to the extremely limited data.

3.1.2.1.   Methodologies applied by Moeck et al. (2020)

The Moeck dataset compiled various observed groundwater recharge rates from 56 small-scale studies, covering the period from 1968 to 2018, through platforms such as Web of Science and Google Scholar by using key research words of 'groundwater recharge', and 'groundwater percolation' (Moeck et al., 2020).

Moeck et al. (2020) applied three approaches to integrate every study and prevent the occurrence of any unrealistic values. Firstly, the authors excluded the recharge rate estimations spanning less than one year to mitigate potential bias arising from seasonal effects and to ensure completeness in annual recharge estimations. Secondly, only direct natural recharge was considered, excluding artificial recharge and the impacts of irrigation practices. Lastly, locations where rivers and streams dominated the recharge rates were excluded in this compiled dataset (Moeck et al., 2020).

Since the recharge data were primarily gathered from different studies, methodologies of recharge estimation were varied in each study, including both physical and chemical approaches. Notably, the chemical tracer method constituted approximately 80% of the estimations, followed by the water table fluctuation method at 5%. The remaining 15% of recharge rates were obtained through modelling, water balance methods, lysimeter, Darcy methods, heat tracer, and geophysical methods. However, it is essential to recognize that the reliability of these estimations was significantly influenced by temporal and spatial scale, which may introduce bias (Moeck et al., 2020).

Moeck et al. (2020) also evaluated and analyzed the relationships between groundwater recharge rate and 17 independent potential predictor variables based on established or hypothesized relationships to groundwater recharge. The 17 variables were further categorized into continuous and discontinuous variables, and continuous variables can take any values within a given interval. The authors evaluated the correlations between groundwater recharge and the continuous variables. These correlations were developed by assessing the percentage of recharge rates exceeding a selected threshold within 14 bins with an equal distribution of observations across the range of each continuous variable. The selected thresholds represented various conditions, reflecting the corresponding recharge rates (Table 3.1).

Table 3.1. Groundwater recharge rates with corresponding conditions (Moeck et al., 2020)

Conditions	GW recharge rates (mm/year)
Hyper-arid	<2
Arid	<20
Semi-arid	<100
Sub-humid	<300
Humid	<500
Tropical wet	>500

3.2. Simulated recharge from the VIC model

This section aims to present the simulated recharge rates from the VIC model, displaying the comparison between the simulated and observed recharge at different scales. Moreover, there is a comparison of the simulated recharge with the PCR-GLOBWB model to ensure the reliability of the VIC results.

Since the VIC model operates at a resolution of a half degree (30arcmin), the results contained 720 columns and 360 rows, representing longitude and latitude respectively, across the entire globe, and generating 259,200 gridded cells with corresponding coordinates. However, we only took into account 67,209 land cells, thus disregarding the rest of the cells associated with oceanic regions.

3.2.1. the VIC simulations vs. the AQUASTAT observations

We initially converted the simulated recharge rates from a gridded scale to a country scale, obtaining the averaged recharge rate for each country (Annex 2, Table A2.2), and visualizing the recharge rates in Figure 3.3.

Average simulated groundwater recharge at country-scale in 1970-2000 from the VIC model

Groundwater Recharge (mm/year)
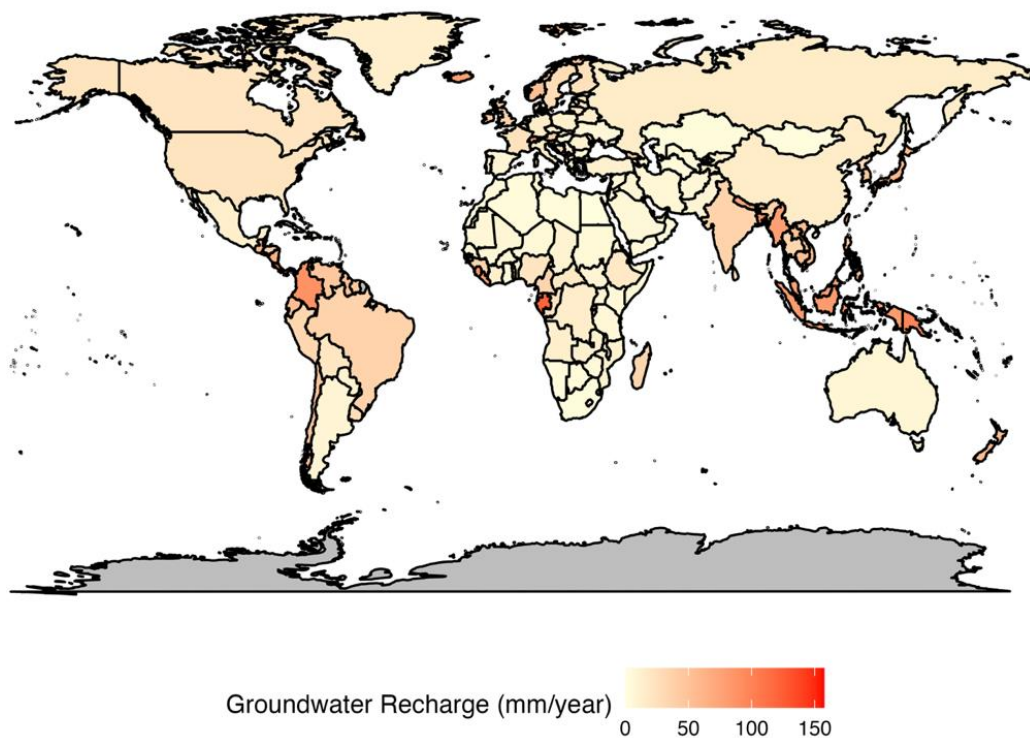
Figure 3.3. Map of the simulated groundwater recharge rates at the country sale according to the VIC model.

To keep the consistency with the AQUASTAT data, we only considered the simulated recharge rates of 169 countries from the VIC model globally with an average recharge of 26.43 mm/year (Table 3.2). Gabon had the highest recharge rate of 121.14 mm/year, while Comoros demonstrated the lowest rate of 0.32 mm/year. Remarkably, the highest and lowest recharge rates occurred both in Africa. Out of the 169 countries, 57 countries (34%) received recharge above the global average, while 112 countries had the recharge less than the average, indicating a similar trend as AQUASTAT observations.

Table 3. 2. The observed and simulated groundwater recharge rates

	Global average (mm/yr)	Max. GW recharge (mm/yr)	Country	Min. GW recharge (mm/yr)	Country
AQUASTAT	145.57	730.1	Costa Rica	0.29	Mauritania
VIC	26.43	121.14	Gabon	0.32	Comoros

In North America, simulated recharge rates did not present a significant difference between Canada and the U.S., while Mexico had slightly less recharge with a light-orange colour. Although countries in Central America do not cover vast territorial space, they were shaded in dark orange to red colour, indicative of comparatively higher recharges in Figure 3.3. The simulated recharge rates followed a similar pattern to AQUASTAT observations (Figure 3.1) in South America, wherein recharge rates were notably higher in the northern regions and gradually dropped away towards the southern areas.

In Africa, with the exceptions of three countries (Gabon, Equatorial Guinea, Sierra Leone) with high recharge rates in Central Africa, the average annual recharge in the northern and southern regions were generally less than 25 mm/year. The countries in Northern Europe displayed a relatively high recharge rate, depicted by shades of orange, with Iceland and Norway standing out as the most prominent examples. Conversely, the remaining European countries demonstrated lower recharge rates in general, except Switzerland, which had an average recharge rate of 73.29 mm/year, ranking as the second-highest recharge rate in Europe, following closely behind Iceland (76.71 mm/year). The island countries attracted the most attention in Asia with vivid orange shades. Additionally, Myanmar, Nepal, Bangladesh, and Japan also displayed a visible orange colour in Figure 3.3, indicating the high recharge rates. As we move towards the northern and central regions of Asia, however, recharge rates gradually declined, aligning with the observations from AQUASTAT (Figure 3.1).

Comparing Figures 3.1 and 3.3, we can observe that the average recharge rates between the simulations and observations shared a similar pattern in some regions. For instance, Central Africa always held a high recharge rate compared to the rest of the African continent; South America followed the trend of higher recharge in northern regions, and gradually dropped to the southern regions; the island countries presented a notable high recharge rate in Asia, and Myanmar was always the most prominent one in both figures. Statistically, the global averaged simulated recharge with 26.43 mm/year was found to be 81.8% lower than the observed recharge rate (145.57 mm/year).

Figure 3.4 and Figure A2.3 (Annex 2) illustrate the underestimation of the simulated recharge rates compared to the observed data. The majority of the points in Figure 3.4 deviate below the identity line, representing the significant differences between the simulated and observed recharge rates existing in most countries where the VIC model underestimated recharge rates compared to the AQUASTAT data. At the coordinate (1e+01, 1e+01), a notable division occurs: all points to its left either aligned closely with or surpassed the identity line which indicates a positive correlation or overestimation, respectively, while nearly all points to its right fell below the identity line which represented an underestimation. This observation suggests that in a few low-recharged countries, the VIC model tended to simulate recharge rates that closely matched with the observed recharge rates. However, as the annual groundwater recharge increased in most countries, the simulated recharge rates tended to diverge from the observations.
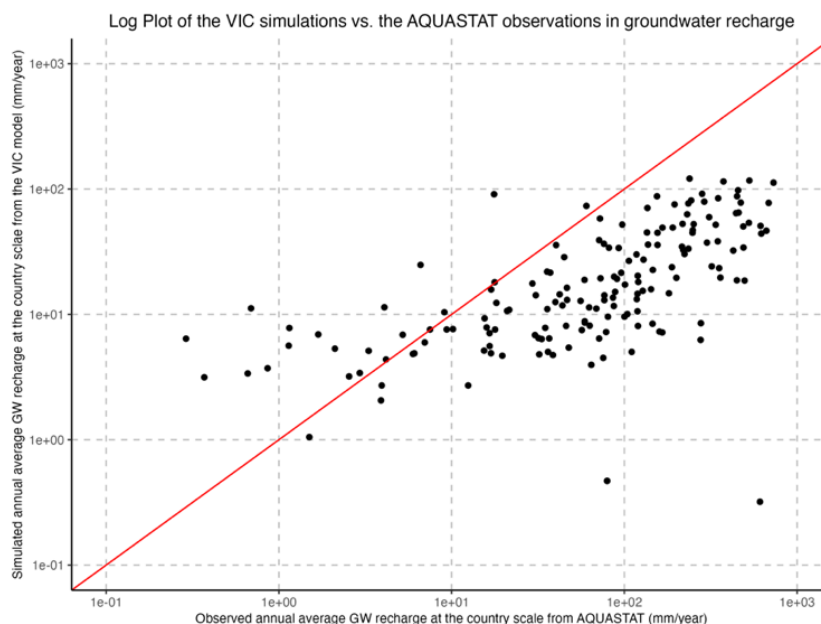
Figure 3.4. The log plot of the simulated VIC recharge and the observed AQUASTAT recharge at the country scale.

3.2.2. the VIC simulations vs. the Moeck data

On the gridded scale, the VIC model had the average recharge rate of 29.6 mm/year, while the Moeck dataset had it of 299.54 mm/year. We converted both the VIC and Moeck datasets into vector scale to generate a scatter plot to analyse their correlations, as shown in Annex 2, Figure A2.4. To enhance clarity, given the density of points at the bottom of Figure A2.4 (Annex 2), we generated a log plot for a better comparison (Figure 3.5). It is evident that the vast majority of points did not align along the identity line, suggesting extensive differences between the VIC simulations and Moeck observations. While some point deviated above the identity line, a greater number of points deviated below it, particularly those densely clustered between 1e+02 and 1e+03 on the axis. Another remarkable observation from Figure 3.5 is the presence of several distinct horizontal lines formed by the clustered points. These lines indicated examples where the observed recharge rates increased, yet the simulated recharge rates were consistently close to one another. Conversely, there were also fewer points with very low observed recharge rates, yet the VIC model indicated high rates, presenting along the y-axis. In general, there is still a trend of underestimation in simulated groundwater recharge compared to the Moeck observations.

Log plot of the VIC simulations vs. the Moeck data observations in groundwater recharge
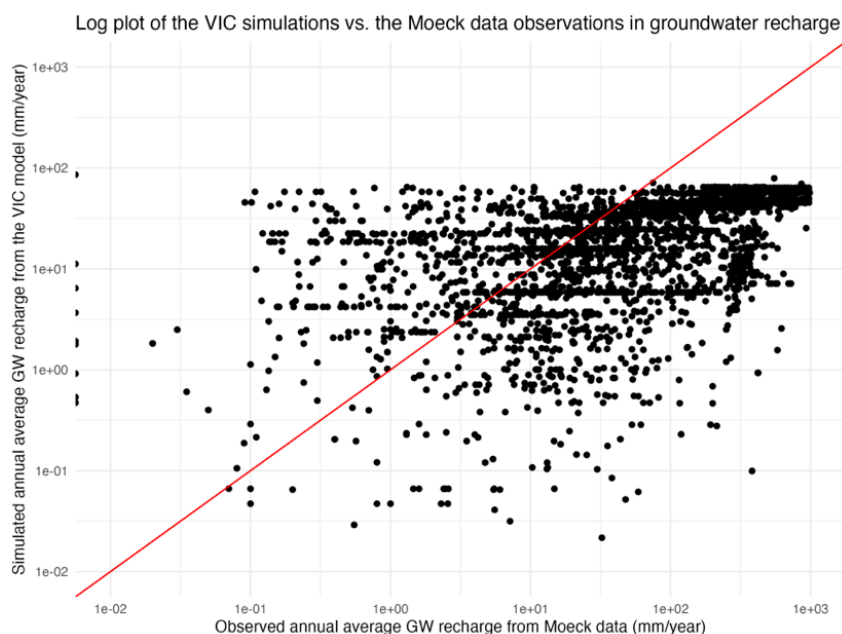
Figure 3.5. The log plot of the simulated VIC recharge and the observed Moeck recharge at the gridded scale.

To facilitate a more comprehensive understanding between the VIC simulations and Moeck observations, we visualized the rasterized recharge data for each dataset, shown in Figure 3.6 and 3.7. Figure 3.6 depicts the simulated groundwater recharge rates with more details at the gridded scale than the country scale (Figure 3.3). In Greenland, coastal regions presented notably higher recharge values with blue and green shades compared to the inland areas, which were greatly shaded in white. While South America generally experienced a decrease in recharge rate from north to south, Figure 3.6 reveals that coastal regions in the southern part still demonstrated high recharge rates with blue and green shades. In Asia, a distinct trend emerged, with recharge rates declining from the southern island countries toward the Northern and Central Asian countries. Notably, the average recharge rate of Myanmar stood out at the country scale in Figure 3.3, but Figure 3.6 shows that its inland central areas showed significantly lower rates with blue shades compared to the coastal high rates with red shades, indicating an uneven distribution of recharge rates. Although the average recharge rate of China at the country scale was not conspicuous with 15.13 mm/year (ranked #112, see Annex 2, Table 2.2), Figure 3.6 depicts pronounced variations that southern regions displayed prominent high recharge rates in green shade, with a distinct trend towards lower rates in the northern regions.
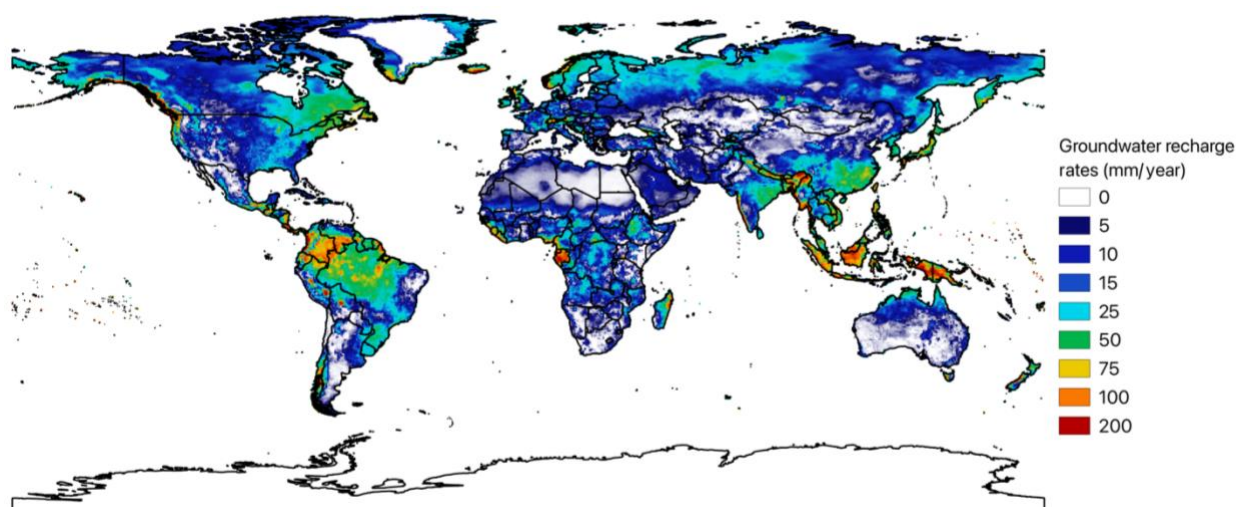
Figure 3.6. Visualization of global simulated groundwater recharge rates from the VIC model at the gridded scale.

However, owing to the limited observed data provided by Moeck et al. (2020), it is challenging to discover an explicit trend of rasterized recharge rate on a global scale in Figure 3.7. Therefore, we chose several pivotal regions to explore more insights between the simulations and observations.
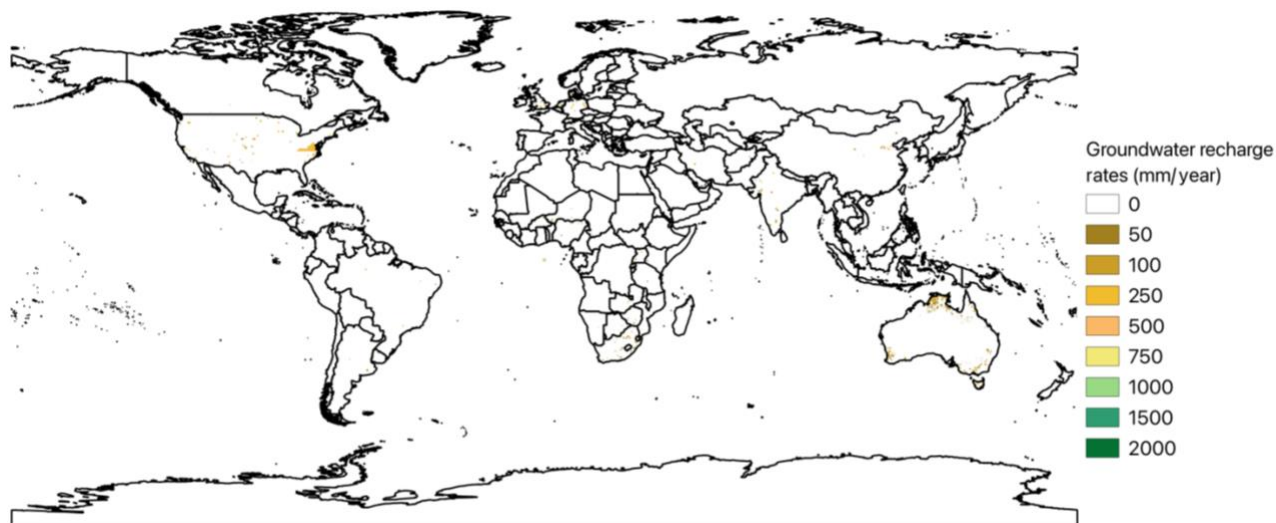
Figure 3.7. Visualization of the global observed groundwater recharge rates from the Moeck dataset at the gridded scale.

Figure 3.8 displays the simulated and observed groundwater recharge rates at the gridded scale in the U.S. Although the observed data was limit, we still can detect the recharge rates in the eastern-central regions were higher than the rates in the Great Plains regions. The simulated recharge rates described a similar spatial distribution from the observations, while the numerical differences are substantial. The simulated recharge presented high recharge rates in the northeast regions, but it gradually decreased from the eastern-central to the southeast region, changing from green to blue shades. The recharge in eastern-central areas did not display a distinct difference compared to the central area. The simulated recharge rates

had high values along the coast in the western regions, while the observed data was too sparse to conclude a convincing trend of recharge rates.
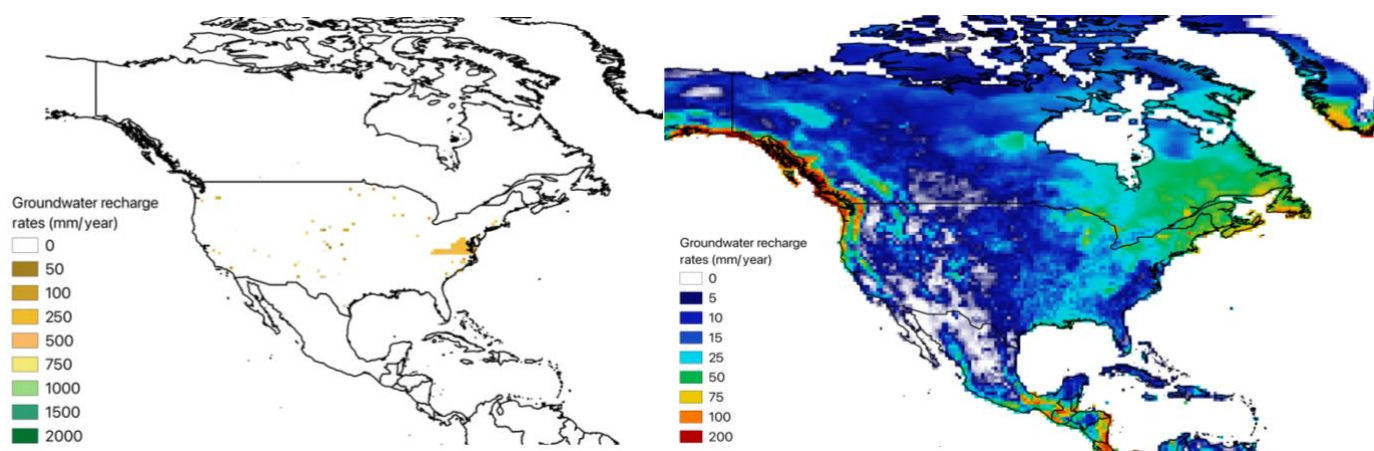
Figure 3. 8.The observed groundwater recharge rates (left) and the simulated groundwater recharge rates (right) at the gridded scale in the U.S.

Figure 3.9 presents the simulated and observed recharge rates at the gridded scale in Australia. Both the observed and simulated recharge rates shared a similar tendency that there were higher recharge rates along the coastal regions than the inland regions.
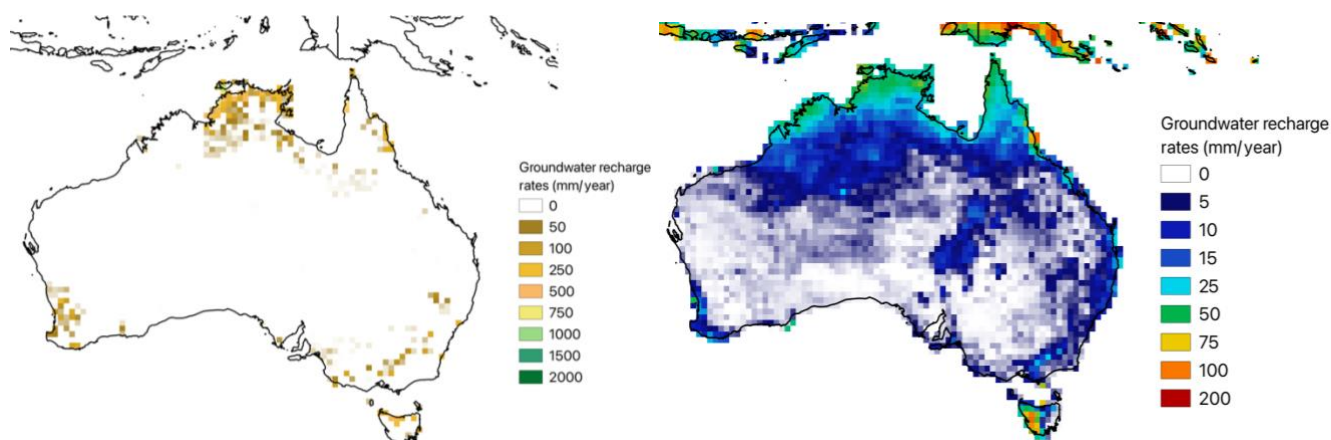
Figure 3.9. The observed groundwater recharge rates (left) and the simulated groundwater recharge rates (right) at the gridded scale in Australia.

3.2.3. The VIC simulations vs. the PCR-GLOBWB simulations

To validate the reasonableness of the groundwater recharge rates generated by the VIC model, we computed a scatter plot to compare to the simulated recharge rates from the PCR-GLOBWB model, shown in Figure 3.10. We note that most points cluster near the lower section of the identity line, especially within the region between (0, 0) and (200, 200). A notable disparity is the presence of the negative recharge rates generated by the PCR-GLOBWB model, while the VIC rates remained consistently positive. Moreover, a vertical line

Study of Global-scale Simulated Groundwater Recharge and Sensitivity Analysis of the VIC Model   28

formed along the y-axis with clustered points, presenting a considerable disparity between the VIC and PCR-GLOBWB simulations: while the VIC recharge rates demonstrated an increase, the PCR-GLOBWB recharge rates remained close to zero across a significant number of gridded cells. Overall, there are minor discrepancies between the two simulated datasets, but they displayed a shared tendency in groundwater recharge rates.
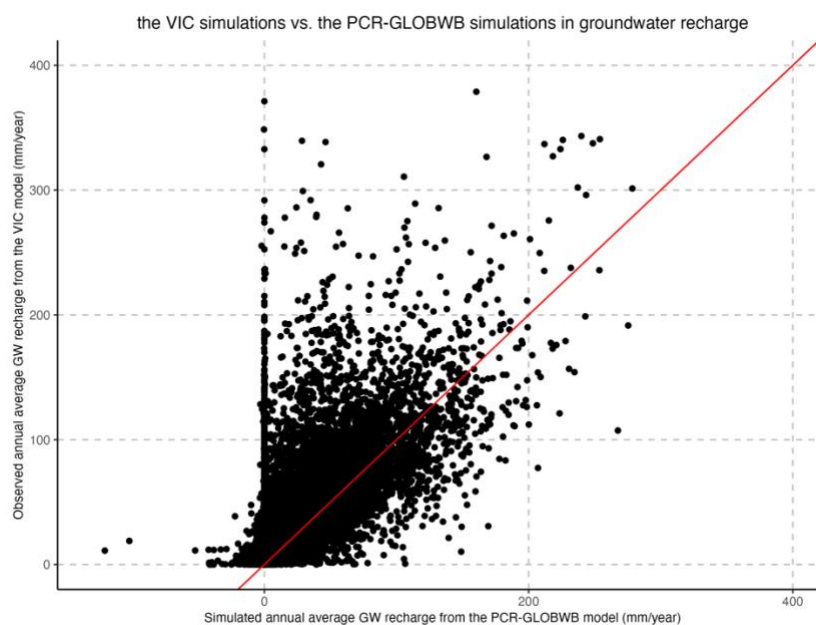
Figure 3.10. The scatter plot of the simulated recharge rates from the VIC and PCR-GLOBWB models at the gridded scale.

3.3. Sensitivity tests from the VIC model

We followed the procedures as described in section 2.4 for the sensitivity tests and we present the results of the groundwater flow exchanges and depths generated from 'recharge factor 1','recharge factor half', and 'recharge factor 2' in this section with associated graphs.

3.3.1. The simulated flow exchange between surface and groundwater

The simulated flow exchange between surface and groundwater presented both positive and negative values in Figures 3.11, 3.12, and 3.13, referring to the inputs of recharge factor 1, recharge factor half, and recharge factor 2, respectively. The positive flow exchange represented the process in which surface water infiltrated into the aquifer, and we named it the river infiltration process. The negative baseflows represented the process by which water flew out of the aquifer, naming as the discharge (baseflow) process. Since the term baseflow is commonly used in various studies (e.g., Arnold et al., 2000; Combalicer et al., 2008; Zomlot et al., 2015; Schilling et al., 2021) to represent the flow exchange, we also use the term 'baseflow' to replace 'the simulated flow exchange between surface and groundwater' for simplification in the rest of the paper.

From the baseflow generated from recharge factor 1, we determined the maximum volume of the river infiltration process was 691,220 m^3/day, while the maximum volume of discharge reached 818,348 m^3/day. The global average baseflow from recharge factor 1 was 9,570 m^3/day, as shown in Table 3.3, where the negative sign represents the discharge process, indicating that groundwater predominantly tended to flow out of the aquifer globally.

Table 3.3. Simulated maximum volumes of re-recharge, discharge, simulated global average baseflows, and percentage differences from recharge factor 1, factor half, and factor 2

GW recharge input	Max. river infiltration (m^3/day)	Max. discharge (m^3/day)	Global average flow exchange (m^3/day)	% difference of global average flow exchange
Factor 1	691,220	(-)818,348	(-)9,570	
Factor half	758,082	(-)587,475	(-)6,201	-35.2%
Factor 2	597,276	(-)1,252,478	(-)15,157	58.4%

Although the maximum volume of water flowing to the aquifer attained approximately 700,000 m^3/day, it is relatively difficult to observe the river infiltration in Figure 3.11, which was shaded in dark red. A notable feature is the vivid red shades in Figure 3.11, locating in the western region of Kazakhstan, Central Asia, representing the daily baseflow was about 0 m^3. In contrast, the remaining global baseflow mostly displayed the discharge process. Remarkably, humid regions still held the highest rates of discharge, particularly in the Amazon Basin, Gabon, and the island countries in Asia, with dark blue clustering. Furthermore, most of arid regions did not provide information about the simulated baseflow, except part of the areas in the Middle East, showing a discharge process with a rate of around 2,500 m^3/day. Taking Australia as an example, we can find that there were higher baseflow along the coast with blue shades, representing the volume of discharge ranging from 5,000 to 20,000 m^3/day. The discharge gradually decreased when moving towards the central areas, ranging from 500 to 2,500 m^3/day, but we can still observe several red shades sporadically, representing 0 m^3/day of the simulated baseflow.
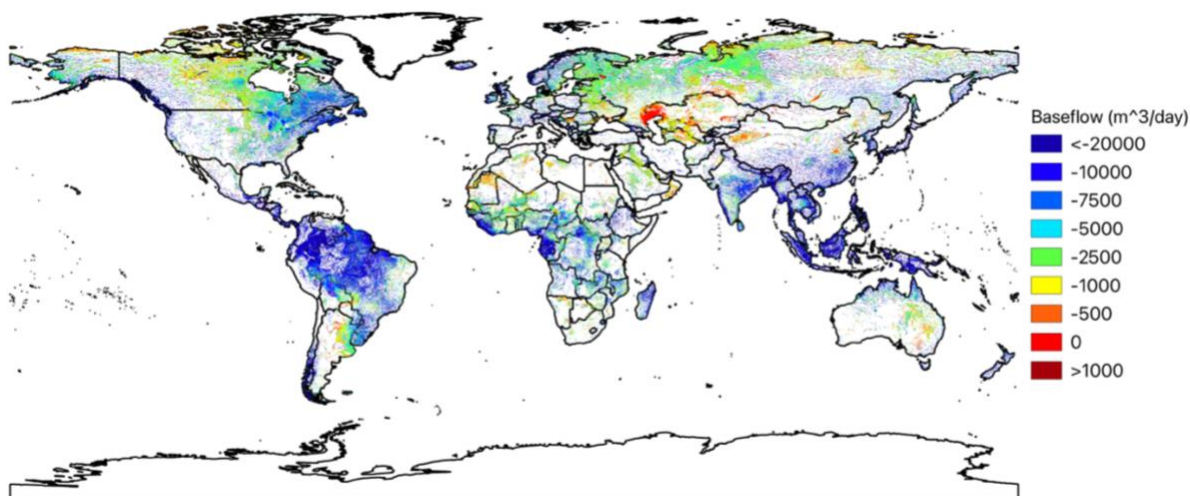
Figure 3.11. Simulated groundwater baseflow from MODFLOW when the input recharge had a factor of one.
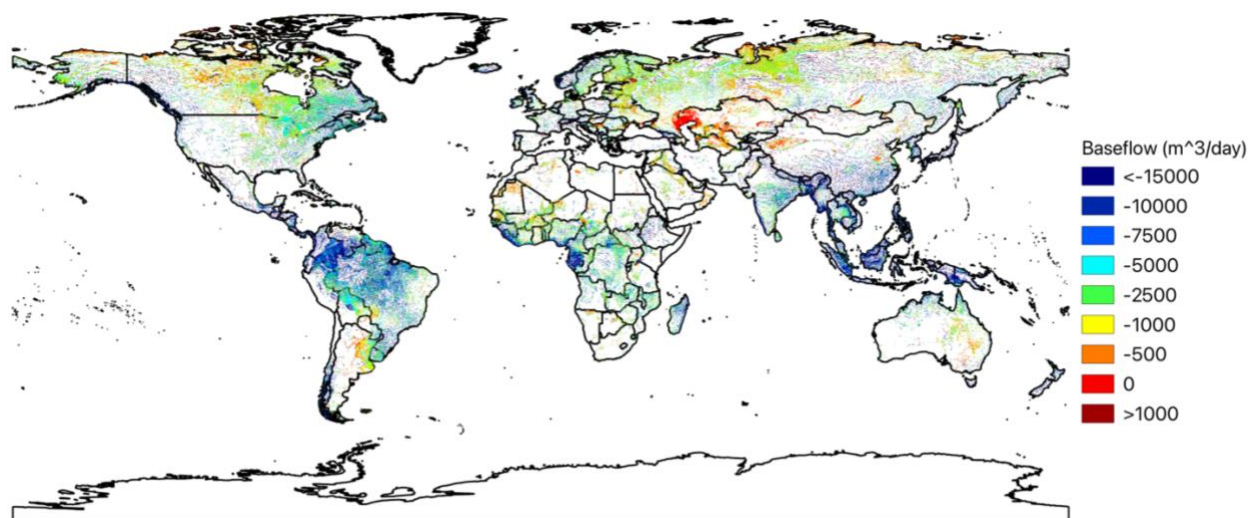
Figure 3.12. Simulated groundwater baseflow from MODFLOW when the input recharge had a factor of half.
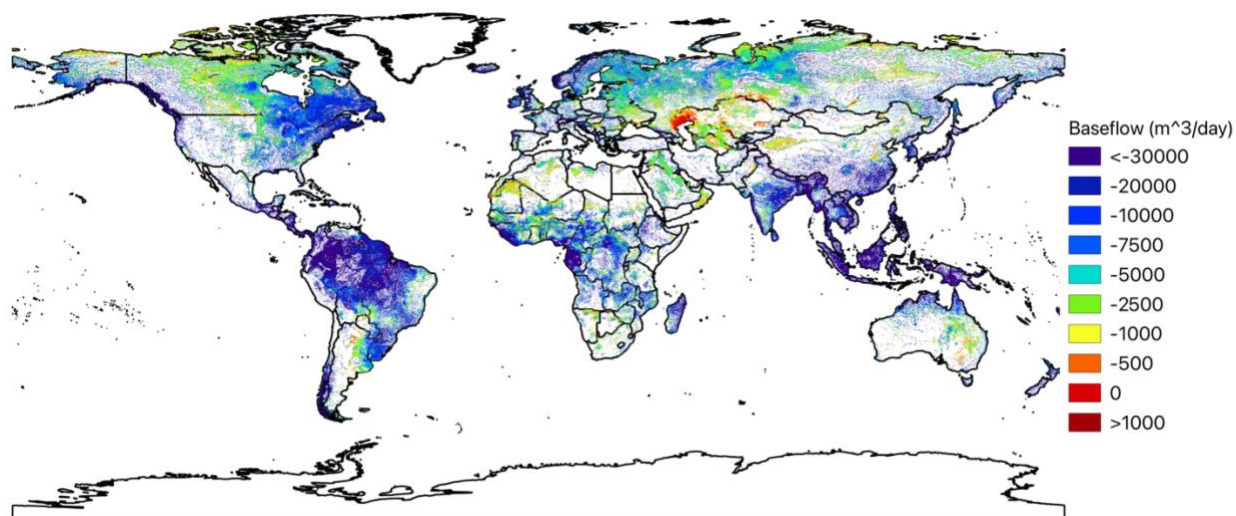
Figure 3.13. Simulated groundwater baseflow from MODFLOW when the input recharge had a factor of two.

When the input recharge had a factor of half in the MODFLOW simulation, we obtained the maximum volume of river infiltration with $758,082 \ m^3/day$, but the maximum volume of discharge decreased to $587,475 \ m^3/day$. The global average groundwater baseflow was $6,201 \ m^3/day$, with a negative sign representing the discharge process, decreased nearly 35% compared to the global average baseflow from 'recharge factor 1' (Table 3.3).

Figure 3.12 shows that the vast majority of regions that were still dominant by the discharge process globally when halved the recharge input, and the location of the river infiltration, shading in dark red, is still difficult to observe in Figure 3.12. Similar to the baseflow from recharge factor 1, the western regions of Kazakhstan were still shaded in a bright red colour, representing the daily groundwater baseflow was around $0 \ m^3$. According to the results of absolute difference (Figure 3.14) between the two simulated baseflows, these regions were also presented in yellow shades, indicating the numerical differences

approached $0\ m^3/day$. Conversely, these regions were shaded in purple in Figure 3.15, representing about 50% relative differences. This result demonstrates that even though the absolute differences between the two simulated baseflows were nearly approaching $0\ m^3/day$ in the western regions of Kazakhstan, the baseflows from the halved recharge were still decreased about by half compared to the baseflow from the original recharge of factor 1.
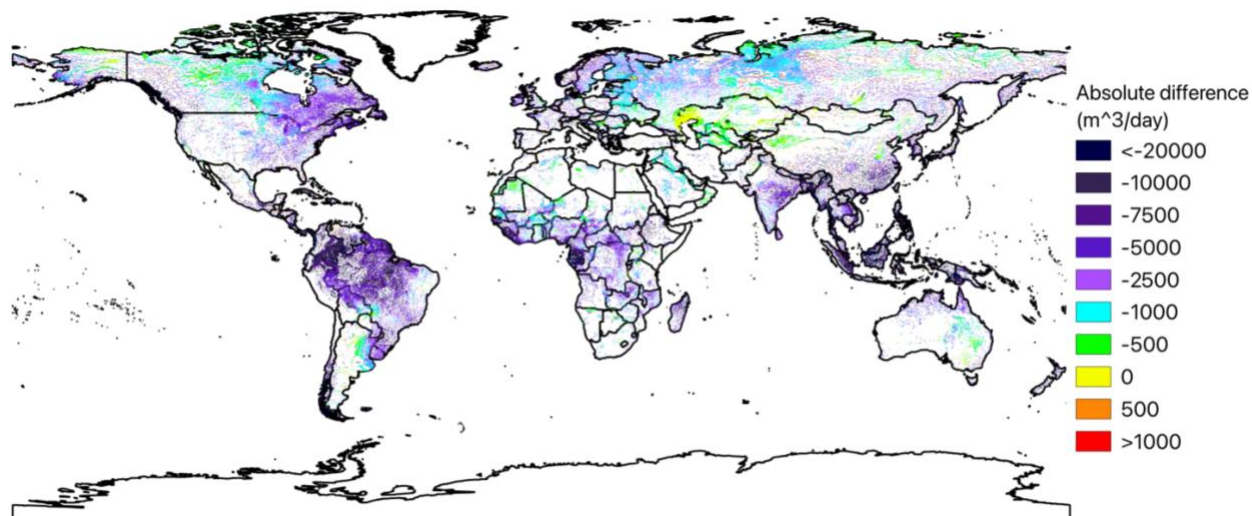
Figure 3. 14. Absolute differences on simulated baseflows between recharge factor 1 and recharge factor half.
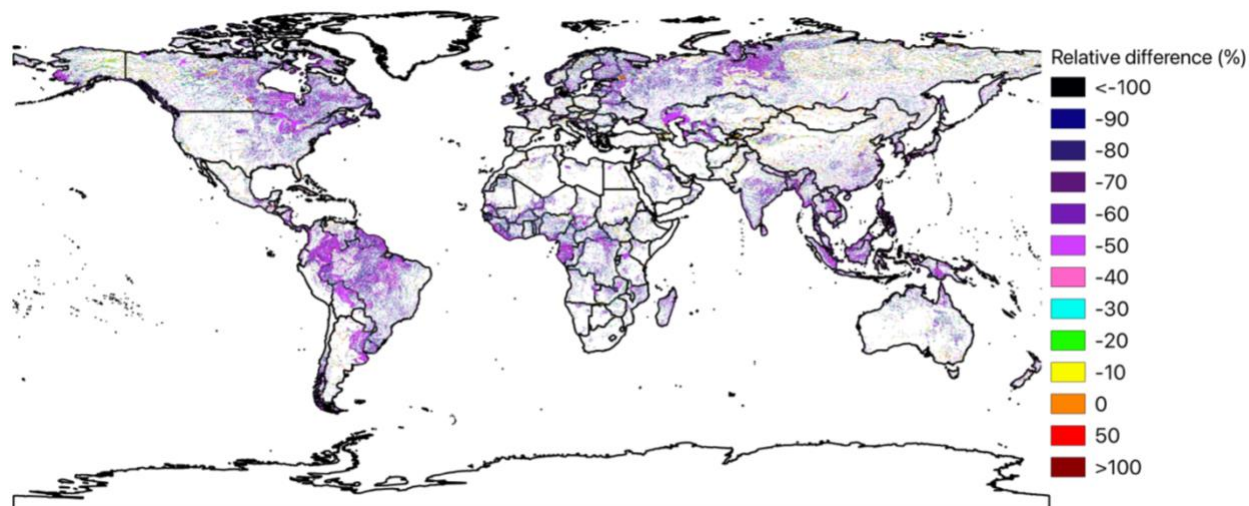
Figure 3. 15. Relative differences on simulated baseflows between recharge factor 1 and recharge factor half.

In the spatial distribution, we observe that humid regions still had a greater volume of groundwater baseflows, mainly the discharge process, shading in dark blue in Figure 3.12. However, a prominent trend of declining presented in humid regions based on the dispersed and lighter shades in Figure 3.12, and the results of absolute and relative differences also supported this tendency. In Figure 3.14, the purple shades were largely located in humid regions, indicating the greatest numerical differences compared to the baseflow from recharge factor 1. The absolute differences in the semi-arid and arid regions were relatively

minor, with green and blue shades of approximately 500 to 1000 m^3/day. According to the results of relative differences (Figure 3.15), we can detect the remarkable purple shades in humid regions again, indicating that baseflow simulated from recharge factor half were about 50% lower than that from recharge factor 1. The disparities in semi-arid and arid regions were relatively small in Figure 3.15, but baseflow were still 10-20% lower than that from recharge factor 1.

When the input recharge got doubled in MODFLOW, we can detect a great change in groundwater baseflow. According to Table 3.3, the maximum volume of river infiltration dropped to 597,276 m^3/day, but the maximum volume of discharge climbed to 1,252,478 m^3/day. The average volume of baseflow shifted to 15,157 m^3/day globally., dominated by the discharge process in which water flew out of the aquifer. Compared to the averaged baseflow from recharge factor 1, the average baseflow from recharge factor 2 increased by approximately 58%.

Figure 3.13 depicts the global distribution of groundwater baseflow simulated from recharge factor 2. We still can observe the western regions of Kazakhstan in red shades, representing a daily baseflow of about 0 m^3, following a similar trend to Figure 3.11 and 3.12. However, we can detect significant changes in humid regions of increasing in discharge volume from darker and denser blue shades with broader coverage area in Figure 3.13. The results from absolute and relative differences ca also support this increased trend of discharge. Figure 3.16 presents absolute differences on simulated baseflows between recharge factor 1 and 2. We can observe the numerical differences reached or even over 30,000 m^3/day in humid regions, such the southern regions of the Amazon Basin, Gabon, coastal regions in Myanmar, regions in Central America, and islands countries in South Asia, shading in bright red. Other humid regions of southern hemisphere also presented high absolute differences, ranging from 10,000 to 20,000 m^3/day with orange and yellow shades, while humid regions in northern hemisphere displayed relatively low disparities, ranging from 500 to 7,500 m^3/day, coloured in purple, blue, and green in Figure 3.16.
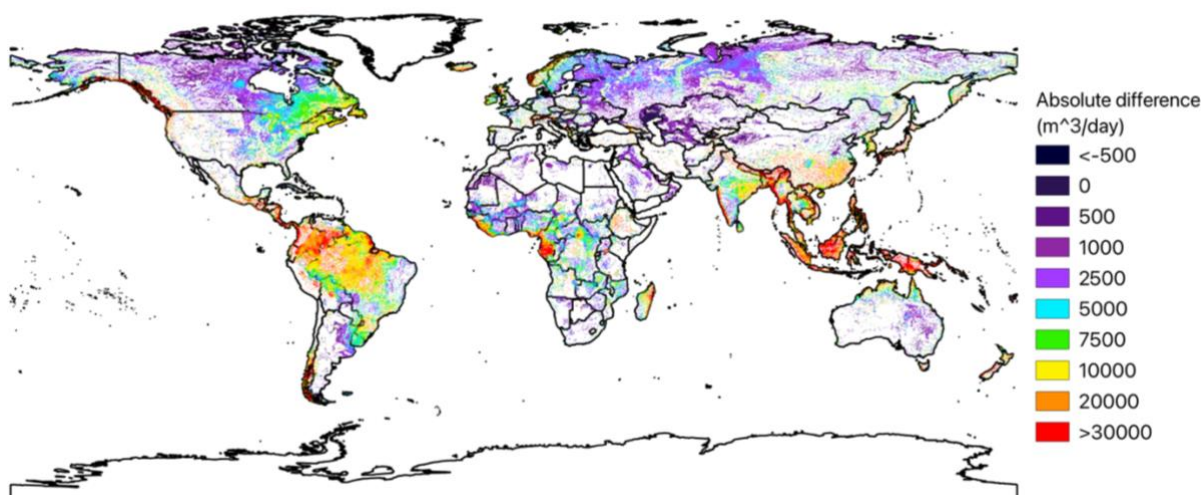
Figure 3.16. Absolute differences on simulated baseflows between recharge factor 1 and recharge factor 2.

Study of Global-scale Simulated Groundwater Recharge and Sensitivity Analysis of the VIC Model   33

Figure 3.17 shows significant relative differences in humid regions, shading in orange and red colours. These differences suggest that simulated baseflow resulting from recharge factor 2 nearly doubled or exceeded double baseflow originating from recharge factor 1. Notably, the western regions of Kazakhstan showed an absolute difference of nearly $0\ m^3/day$, but these regions were shaded in a prominent red in Figure 3.17, representing baseflow had doubled or more than doubled the baseflow simulated from recharge factor 1. Even though the other coloured cells were relatively dispersed in Figure 3.17, we still can determine that many of them were shaded in dark purples, indicating an increase in baseflow about 10-40%.
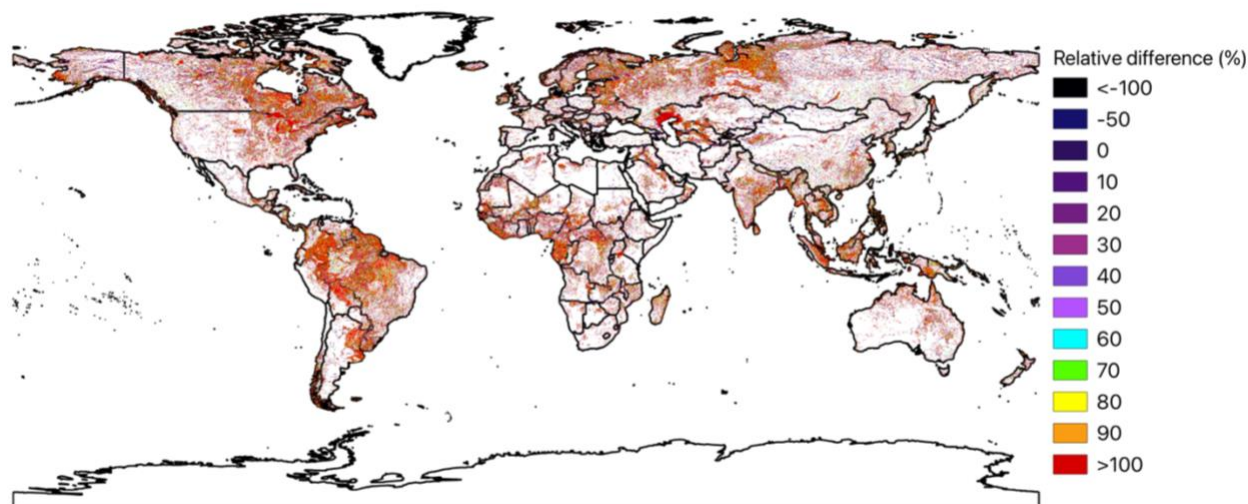
Figure 3.17. Relative differences on simulated baseflows between recharge factor 1 and recharge factor 2.

Figure 3.18 a), b), c) show the histograms of the distribution of the simulated groundwater baseflows with different recharge inputs, firmly supporting the correlation between recharge and baseflow dynamics: the volume of baseflow increases as recharge increases, while decreasing recharge leads to a corresponding decrease in the volume of baseflow. We can observe that most data were distributed negatively, representing the dominance of the discharge process that water flew out of the aquifer. When the recharge halved, the frequency drastically decreased of the breaks between -500 and -5000 m^3/day, as shown in Figure 3.18 a) and b). Conversely, the frequency of each break prominently increased in the range of (-10,000, 0) m^3/day when the recharge increased by 100%, presented in Figure 3.18 b) and c).
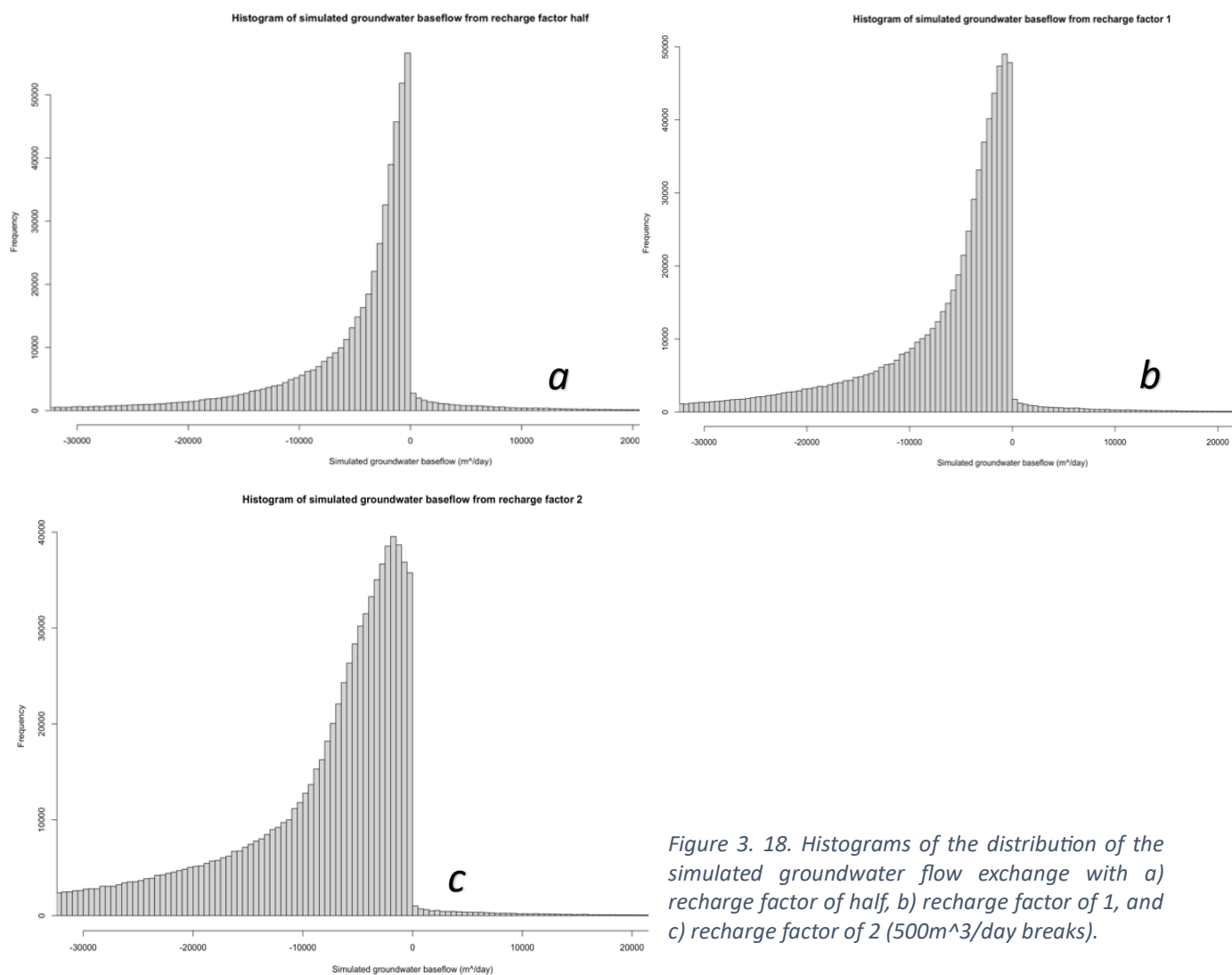
Figure 3. 18. Histograms of the distribution of the simulated groundwater flow exchange with a) recharge factor of half, b) recharge factor of 1, and c) recharge factor of 2 (500m^3/day breaks).

3.3.2. The groundwater depths

According to Eq.2 from section 2.4, we acquired and visualized the groundwater depths from each sensitivity test with different recharge inputs in Figures 3.19, 3.20, and 3.21. Each figure presents both positive and negative values in groundwater depths, in which positive values represented the depths above the ground, while negative values referred to water depths below the ground.

Figure 3.19 depicts the simulated groundwater depths with inputs of recharge factor 1. We can observe that semi-arid and arid regions were mostly shaded in red and dark red, representing the groundwater depths were approximately or greater than 200 m above the ground. In contrast, humid regions were heavily shaded in blue, referring about 0 m of the depths, indicating shallow groundwater in humid regions which water tables got closer to the land surface.
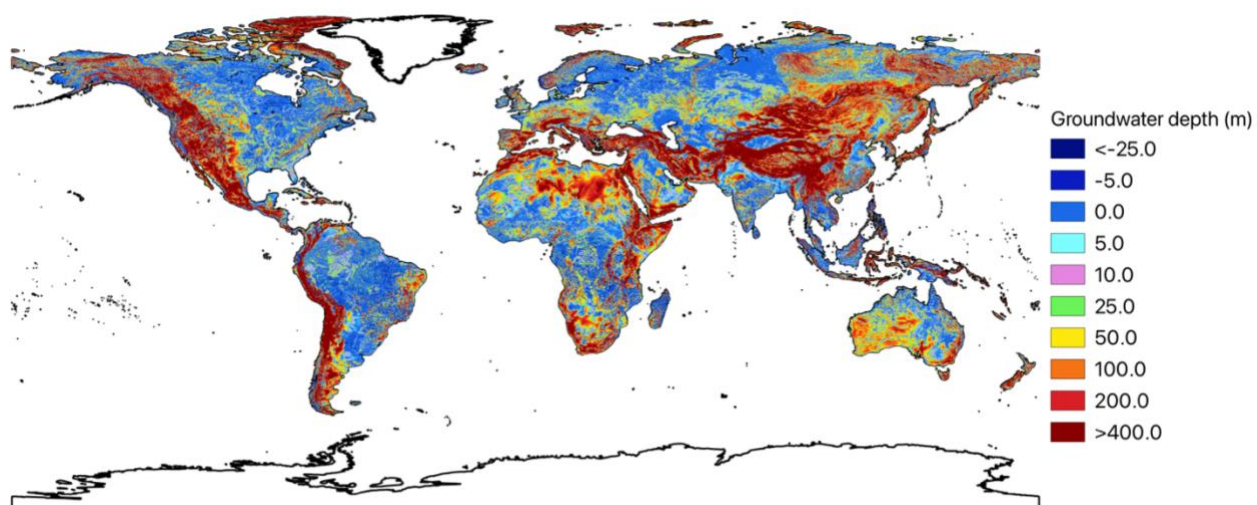
Figure 3.19. Simulated groundwater depths from MODFLOW when the input recharge had a factor 1.
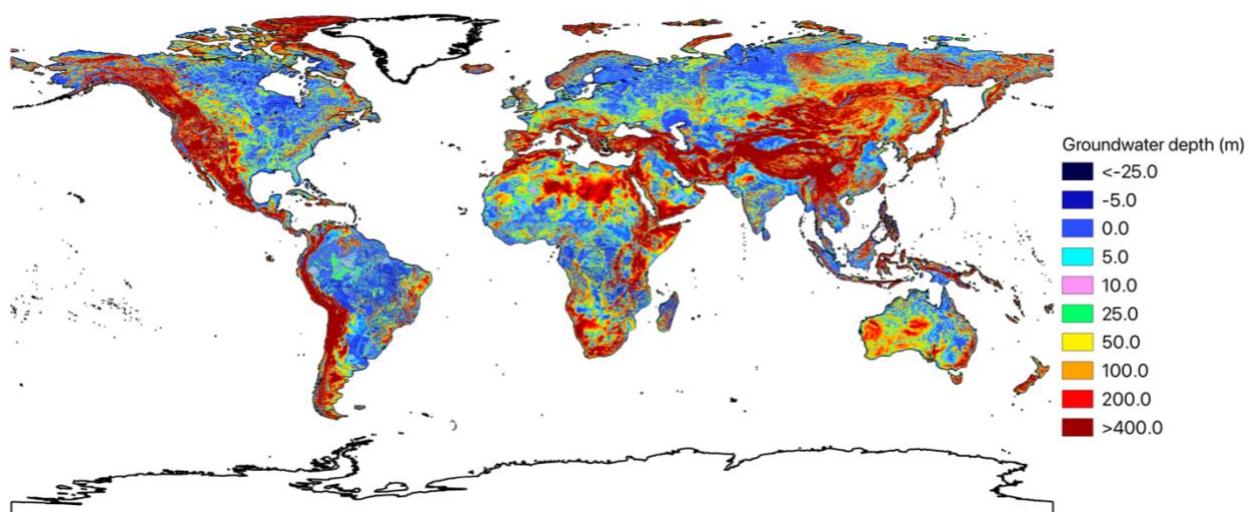
Figure 3.20. Simulated groundwater depths from MODFLOW when the input recharge had a factor half.
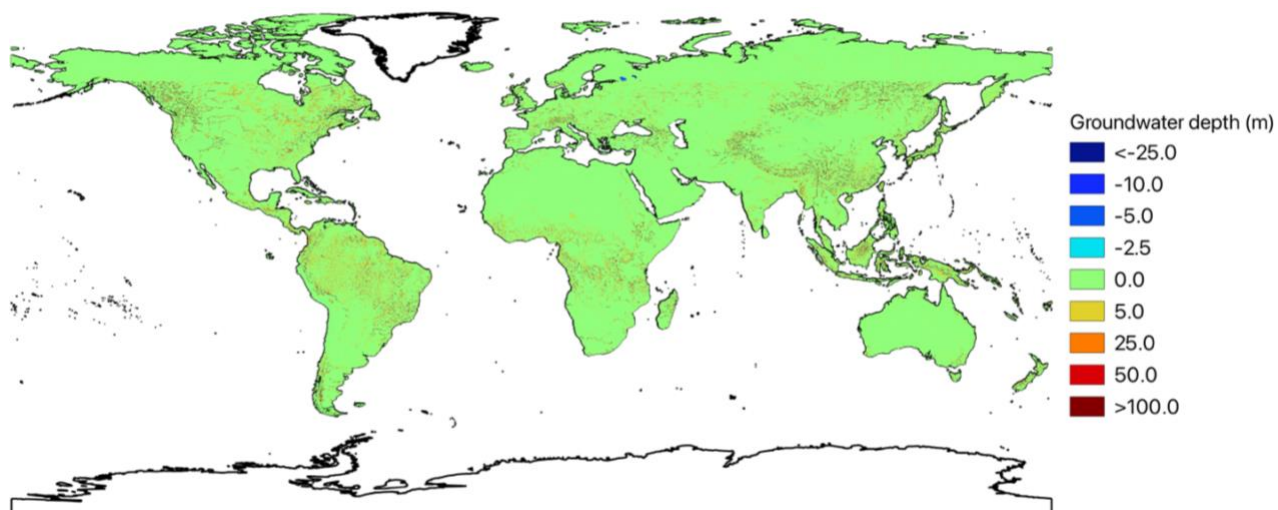
Figure 3.21. Simulated groundwater depths from MODFLOW when the input recharge had a factor 2.

When we decreased the recharge input by half, the simulated groundwater depths did not present a great spatial difference compared to the depths from recharge factor 1, as shown in Figure 3.20. Arid and semi-arid regions were still coloured red, representing positive groundwater depth exceeding 200 m. Humid regions were also shaded in blue colour, representing shallow groundwater with depths near 0 m.

According to absolute differences of the simulated groundwater depths between recharge factor 1 and half, there are minimal numerical differences existing in humid regions, shading in blue with about 0 m in Figure 3.22. However, Figure 3.23 displayed notable disparities in humid regions where were shaded in blue and represented roughly -50% differences in groundwater depths based on the results from relative differences. This reduction revealed shallower groundwater depths in humid regions when decreased the recharge input, accompanied by an elevation of water table, bringing it closer to the land surface.
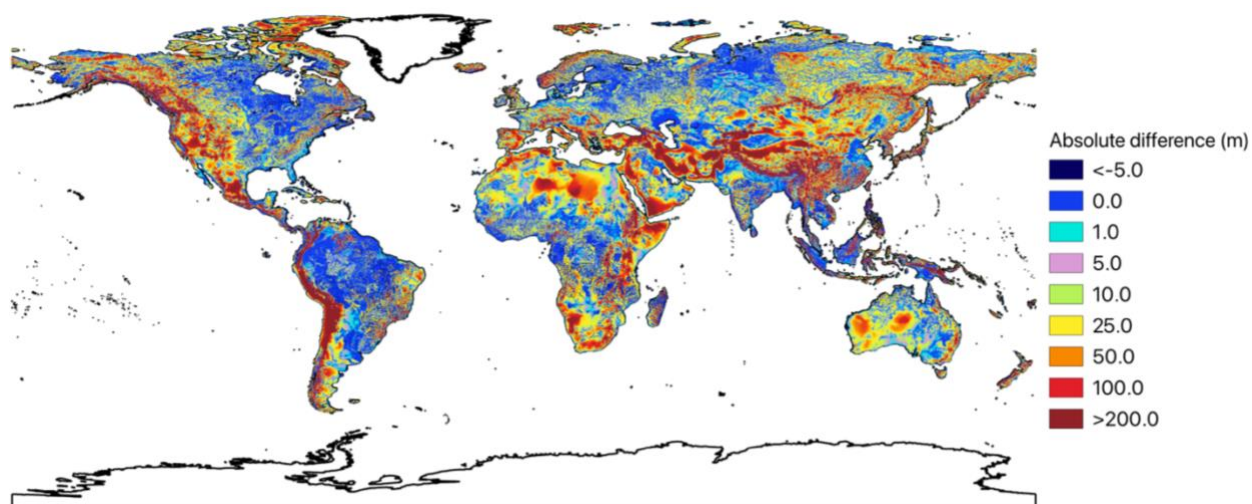
Figure 3.22. Absolute differences on simulated groundwater depths between recharge factor 1 and recharge factor half.
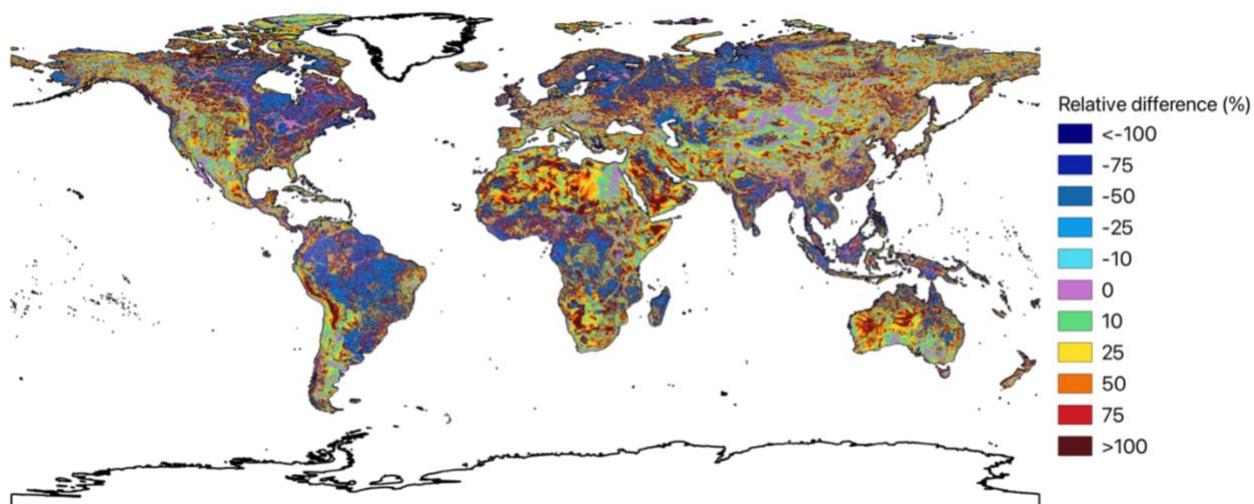
Figure 3.23. Relative differences on simulated groundwater depths between recharge factor 1 and recharge factor half.

The greatest contrasts in absolute differences (Figure 3.22) mostly occurred within arid and semi-arid regions, highlighted in dark red, representing more than 200 m difference numerically, particularly in the Andes Mountains and Himalayas Mountains. Similarly, relative differences within these regions (Figure 3.23) also presented substantial disparities, with dark red shades indicating differences exceeding 100%. Since arid and semi-arid regions had positive values of groundwater depths in Figure 3.20 which represented the depths above the ground, the over 100% relative differences indicated an increase in groundwater depth with less water received in the aquifer.

When the input recharge had doubled in MODFLOW, the simulated groundwater depths displayed a great change in the spatial distribution, as shown in Figure 3.21. At first glance of the map, the entire map was almost dominated by the presence of green, representing groundwater depths around 0 m. This observation highlights that not only humid regions but also semi-arid and arid regions experienced shallower groundwater depths, with water table moving closer to the land surface, and the entire land surface will be covered by water. Upon closer regional observations, variations existed in humid regions. For example, we can find yellow and orange shades along the rivers in the Amazon Basin, shown in Figure 3.24 a). representing groundwater depths ranging from about 5 to 25 m above the ground. We also can find the dark red shades in some mountainous regions to represent a greater groundwater depth, such as the Rocky Mountains, Andes Mountains, and Alps, as shown in Figure 3.24 a), b), c).
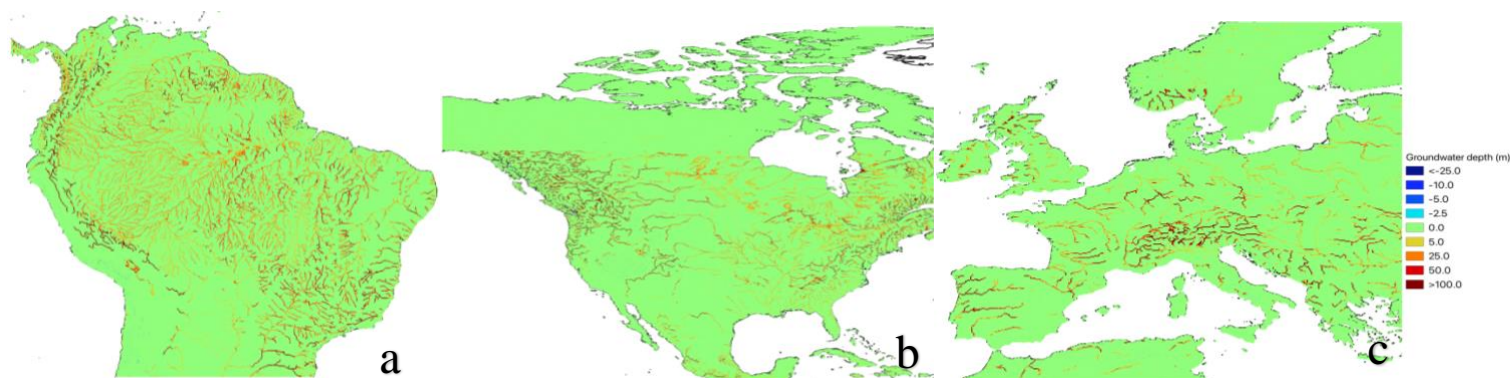
Figure 3.24. Simulated groundwater depths from MODFLOW when the input recharge had a factor 2 with zoom-in maps of (a). the Amazon Basin in South America, (b). the Rocky Mountains in the U.S., (c). the Alps in Europe.

Figure 3.25 displays absolute difference of the simulated groundwater depths between recharge factor 1 and 2. We can detect limited numerical differences in humid regions which were shaded in orange. The most substantial numerical differences occurred mainly in arid and semi-arid regions, as well as in the regions of southern Europe and southern Asia with dark blue shades, representing the exceeding differences of 100 m. This trend indicates a consistent rise in the water table levels in these regions.
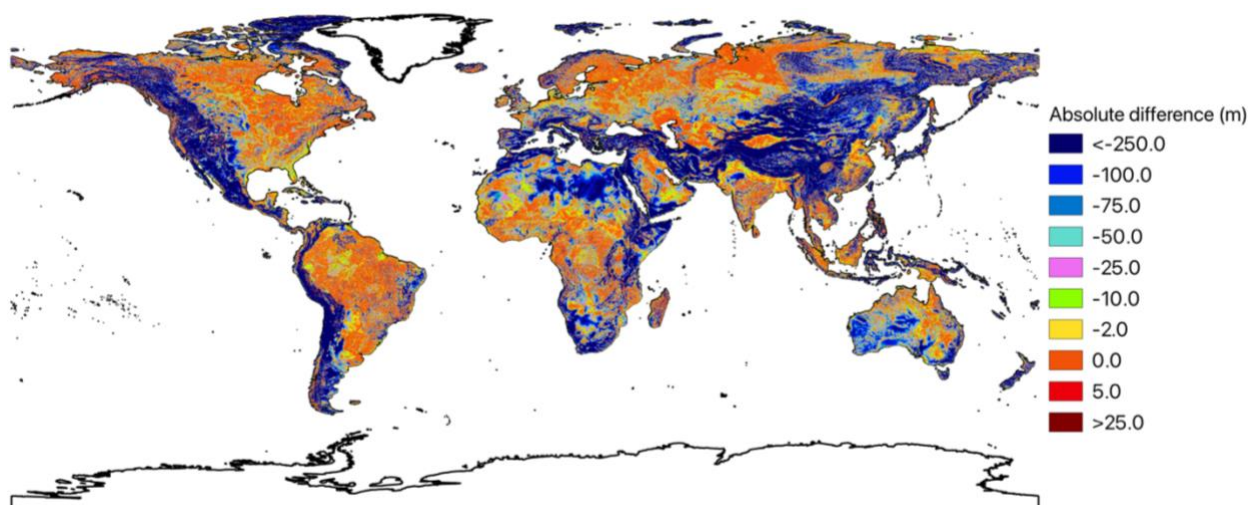
Figure 3.25. Absolute differences on simulated groundwater depths between recharge factor 1 and recharge factor 2.

Figure 3.26 shows relative differences of the simulated groundwater depths between recharge factor 1 and 2. The entire map was almost covered by the blue shades, representing at least 100% differences in groundwater depths between two simulations. This observation indicates that the water table levels increased, moving closer to the land surface, and groundwater became shallower at the global scale. Similar to the map of simulated groundwater depths from recharge factor 2 (Figure 3.21), it is difficult to observe the variations in relative differences in the massive blue shades. However, the preeminent bright green can be observed in the Great Lakes region, illustrating relative differences approaching 0%, suggesting the minimal change in groundwater depths. Furthermore, we can detect smaller relative differences in groundwater depths along the rivers when we have closer regional observations, such as in the Amazon Basin and island countries in South Asia, with pink and bright blue shades, ranging the differences about 10 to 25%.
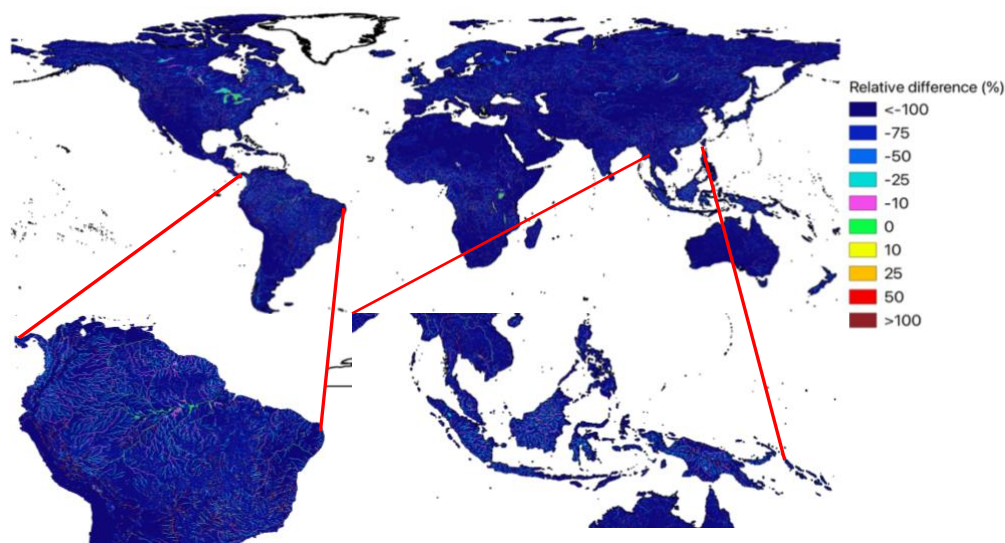
Figure 3.26. Absolute differences on simulated groundwater depths between recharge factor 1 and recharge factor 2.

Figure 3.27 a) and b) show histograms depicting simulated groundwater depths resulting from recharge factors of half and 1, respectively, revealing a similar pattern in data distribution. However, we still can detect a reduction in frequency from over 5e05 to about 4e05 in the interval of (-20, 0) m when decreased recharge. When we modified the recharge by increasing 100%, the pattern of data distribution is completely different, as shown in Figure 3.27 c). Almost all data were located in the intervals of (-20,0) m and (0, 20) m. This shift indicates a decline in the simulated groundwater depths, reflecting shallower groundwater globally and aligning the results from Figure 3.21.
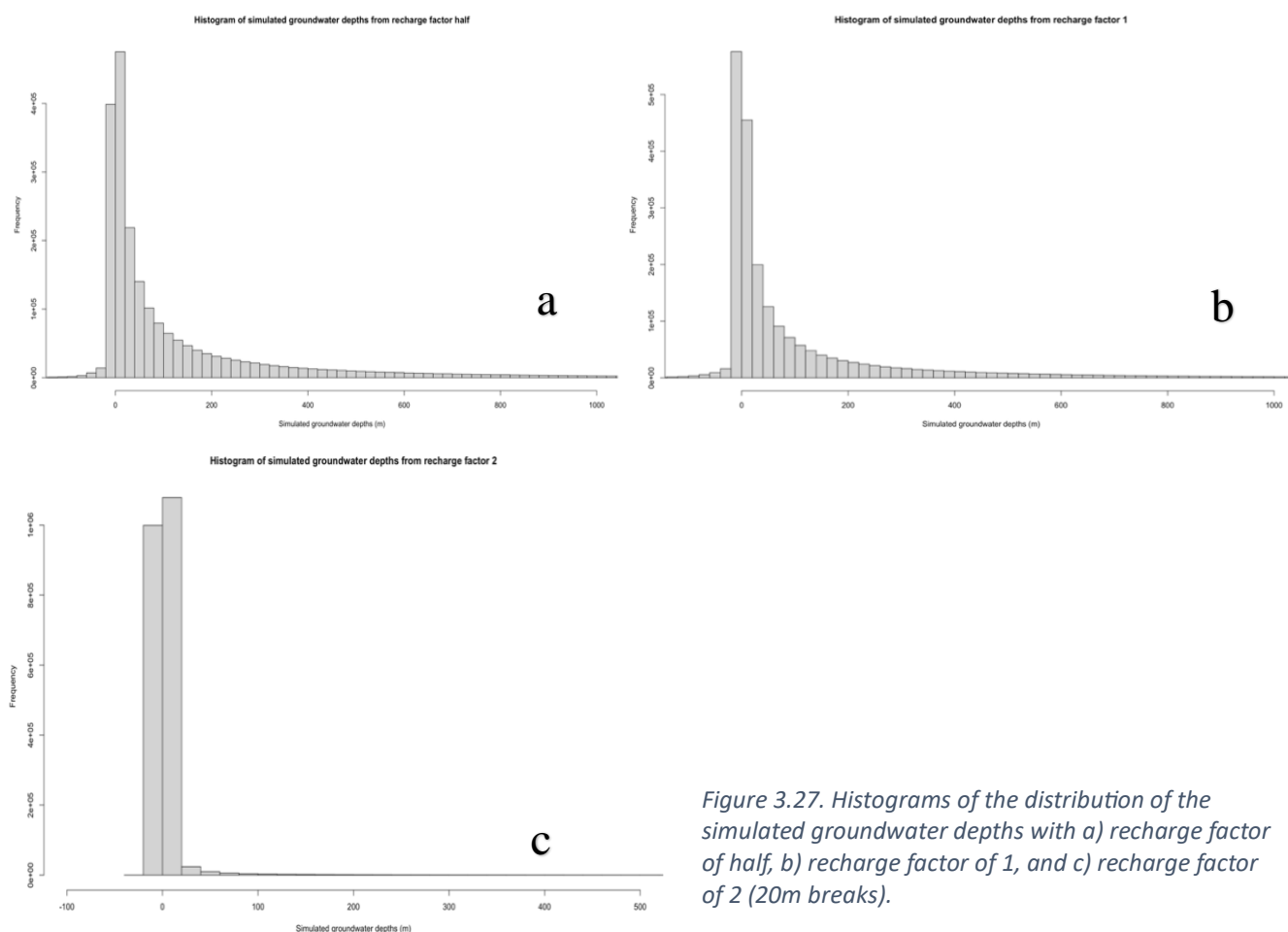
Figure 3.27. Histograms of the distribution of the simulated groundwater depths with a) recharge factor of half, b) recharge factor of 1, and c) recharge factor of 2 (20m breaks).

Chapter 4. Discussion

The chapter concentrates on discussing the key finding providing the potential causes from the results. Moreover, this chapter also discusses the potential errors or missed processes we had during the model simulations, as well as the limitations on global-scale hydrological models, and providing subsequent recommendations for future studies.

4.1. The observed and simulated recharge data

In this study, we focused on two observed recharge datasets at the global scale: the AQUASTAT dataset which has been extensively used by many well-known organizations (FAO, n.d.), and the Moeck dataset which is the most updated observations from reliable sources.

We conducted comparisons of the simulated recharge from the VIC model against each dataset on the country and gridded scales. Our findings illustrated that the VIC model simulations significantly underestimated groundwater recharge rate and the differences of the global average reached over 80% with each observational dataset. This result agreed with the findings of Berghuijs et al. (2022) who reported a general underestimation of half by global-scale hydrological models. However, the VIC model simulations also indicated an improvement in recharge estimation when comparing to other hydrological models, such as PCR-GLOBWB.

Although the VIC model still presented an underestimation of groundwater recharge, we should not ignore the limitations of the comparable dataset. Some studies (Döll et al., 2009; Mohan et al., 2018; Moeck et al., 2020) question the reliability of the AQUASTAT dataset owing to its insufficient clarifications in data acquisition, and we raise similar concerns after exploring their methodologies. One considerable observation is that the original volume of annual groundwater recharge remained constant for most countries and regions from 1970 to 2000 according to the AQUASTAT platform. The constant recharge volumes over 31 years are likely unrealistic, given the inevitable fluctuations in annual precipitation for most countries and regions (Girvetz et al., 2009; EPA, 2022). Furthermore, a remarkable divergence was observed in North America, where the recharge rates were largely distanced between the border-connected countries Canada (37.22 mm/year) and the U.S. (146.12 mm/year). One possible reason for this difference could be the consideration of irrigation practices in groundwater calculation that the irrigation return flow can contribute to an increase in groundwater (Willis & Black, 1996; Han et al., 2017), given that the U.S. has significantly larger irrigated agricultural fields compared to Canada (FAO, n.d.). Unfortunately, there is still a lack of information from AQUASTAT related to such divergences, increasing the uncertainties of its original data source, and decreasing its reliability as observational data for model validation. However, we acknowledge the significance of the AQUASTAT observed dataset to global groundwater recharge, particularly for the previous studies when the observational data were scarce, but it

would be premature and less convincible to label this dataset as entirely unreliable because our evaluation was hindered by the absence of crucial data-sourcing information from AQUASTAT, and we still lack other comprehensive and comparable observational groundwater recharge data on a global scale to identify the accuracy of the AQUASTAT data.

Unlike the AQUASTAT dataset, the compiled Moeck observational data provided robust references regarding the data collection, thereby increasing its reliability as observational data for model validation. Although the VIC model underestimated the average global recharge rate (29.6 mm/year) nearly 90% compared to the Moeck dataset (299.54 mm/year), we should not neglect that the Moeck dataset is still dominated by low recharge rates that most observed data points had rates between 0 and 20 mm/year, also proved by the histogram of the Moeck data distribution (Annex 3, Figure A3.1), while the high averaged global recharge rate was resulted from few data points which exceeded 500 mm/year (Moeck et al., 2020). Therefore, only focusing on the averaged global groundwater recharge rate between the simulations and observations to conclude that global-scale hydrological models underestimate groundwater recharge by half or even more (such as the comparisons from our study and Berghuijs et al., (2022)) cannot provide a comprehensive depiction of the simulated outcomes. In addition, even though Berghuijs et al. (2022) presented a closer simulated average recharge rate compared to the observational averaged recharge rate, their study exclusively focused on the aridity index, while there is a myriad of factors interconnecting the recharge rate. Consequently, the empirical approach to estimating groundwater recharge remains inadequate to fully grasp the complexities inherent in the groundwater system.

4.2. Model sensitivity

When we simulated groundwater baseflow using the original recharge of factor 1, notable discharges were observed, especially concentrated in humid regions, including the Amazon Basin, various island countries in Asia, and the country of Gabon in Africa. Upon adjusting the recharge input, we observed the most substantial changes still occurred in humid regions where groundwater discharge diminished with the decline of recharge, and it escalated with higher recharge accordingly, but changes in baseflow were very limited in hyper-arid regions. These findings suggest that the VIC model exhibited greater sensitivity in humid regions that had abundant precipitation since the model only considers precipitation contributing to groundwater recharge. In contrast, the VIC model is less sensitive in hyper-arid regions owing to less precipitation received, aligning with the challenges of modelling groundwater recharge in arid and semi-arid regions presented by Al-Muqdadi et al. (2020). Moreover, these findings corroborate the statement that recharge dynamics are significantly influenced by climate aridity (Berghuijs et al., 2022) because precipitation acts as the only consideration in recharge simulations. Specifically, humid regions tend to experience greater precipitation, leading to lower aridity, thereby facilitating higher rates of recharge, and

resulting in increased discharge. Conversely, aridity increased in semi-arid and arid regions owing to less precipitation, contributing less recharge, and resulting in less baseflow. Furthermore, reiver discharge is another important parameter we need to notice in the baseflow simulations. We applied the simulated averaged river discharge of July from the PCR-GLOBWB model as the boundary condition in determining groundwater baseflow. However, this approach has its potential limitations that the averaged river discharges of July are usually higher than the rest of the year in the northern hemisphere (Holmes et al., 2021), which can introduce significant differences into the simulated baseflow (Döll & Fielder, 2008; Berghuijs et al., 2022). In addition, the applied river discharge was also the simulated outcome from the PCR-GLOBWB model. Since we proved that the PCR-GLOBWB model underestimated groundwater recharge compared to the VIC model, there is a potential underestimation in river discharge as well.

The simulated groundwater depths displayed shallow groundwater in humid regions with the original recharge of factor 1, and greater groundwater depths occurred in semi-arid and arid regions. When we decreased the recharge by half, the simulated groundwater depths did not present a great spatial difference in general, and the numerical differences were limited, particularly in humid regions. When we increased the recharge by 100%, we obtained substantial changes in groundwater depths, with depths approaching approximately 0 m in the vast majority areas worldwide, suggesting a global trend towards shallower groundwater levels, with water tables moving near to the land surface. Under this situation, water would flush over almost every piece of land, including semi-arid and arid regions, which is unrealistic. This impractical result showed that the VIC model was not effective in simulating groundwater depth when only increasing the single parameter of recharge, suggesting that we missed or underestimated some important processes or factors in the model simulations. For instance, shallow groundwater reflects high water tables and more stored water in the aquifer, so it is reasonable to assume that we underestimated the hydraulic conductivity in the simulations, resulting in insufficient water drained from the aquifer and leading to high water tables. Besides hydraulic conductivity, inaccurate estimations of the parameters of the aquifer could also contribute to the unrealistic groundwater depths. Therefore, based on the results from the sensitivity tests, especially the simulated depths from the doubled recharge, we do not fully agree with the findings from Berghuijs et al. (2022), and it is sceptical that hydrological models underestimate the groundwater recharge worldwide.

4.3.   Recommendations for future studies

According to our findings and analysis, we propose several suggestions for further investigations in groundwater recharge simulations.

It would be beneficial to conduct several additional sensitivity tests for groundwater baseflows and depths, using factors such as 0.75 and 1.5. In this study, we only simulated the baseflows and depths with

factor half, 1, and 2, limiting our ability to fully understand the variations resulting from each recharge factor. For example, while we observed substantial differences in the simulated groundwater depths between the recharge factor of 1 and 2, the lack of testing at an intermediate factor, such as 1.5, hinders our confidence in attributing the differences solely to the adjustment of the single parameter. Therefore, multiple tests with different factors can help the researcher further target on the key underestimated or missed processes or factors in the simulations.

Furthermore, adjusting more parameters in the simulations rather than focusing on a single one. Groundwater is a sophisticated system that involves numerous factors to shape its behaviour and characteristics. Our results showed that only changing recharge cannot help us fully understand the performances of the model. Therefore, we also need to think about the adjustments on other parameters in the system, such as hydraulic conductivity, aquifer properties, or the variables which correlate to recharge tested by Moeck et al. (2020), including topographic wetness index, vegetation, etc. Meanwhile, including the calculation of capillary rise and percolation will also increase the accuracy of estimating groundwater recharge.

Another remarkable consideration that we missed in the updating VIC-WUR model is the anthropogenic activities, especially the agricultural activities and urbanization (Han et al., 2017). For instance, irrigation practices can generate return flow that can increase the recharge rates in many semi-arid regions (Willis & Black, 1996; Han et al., 2017), while continuous urbanization changes the original water balance and modify the traditional recharge mechanism, resulting in the change of recharge rates diversely (Sharp, 2010; Han et al., 2017). Therefore, with the expansion of agricultural practices and urban development, the influence of anthropogenic activities on groundwater recharge becomes more considerable.

Since reliable observational recharge data are still scarce on a global scale, future studies may benefit from focussing simulations on the regional scale, where have sufficient observational data, facilitating a more robust and convincing model validation process. A thorough model validation can provide more details of the performance of the model through the analysis, enabling us to pinpoint weaknesses in the simulations effectively and enhance the model's reliability with the targeted disadvantages subsequently.

Although it is important to improve the reliability of the hydrological models no matter at the regional or global scale, it is also significant to obtain more reliable observational data in groundwater recharge because every observational recharge is valuable owing to the difficulties of the direct measurements. Hence, large organizations can create a shared platform to invite researchers and national organizations to contribute their observed recharge data with detailed explanations of methodologies, keeping the consistency of data source and assisting the model validation and development for future studies.

Chapter 5. Conclusion

This study focuses on the evaluation of groundwater recharge from the existing observed datasets and the simulated results from the VIC model, with the aim of assessing the reliability of the VIC model in groundwater recharge simulations at the global scale. In addition, sensitivity tests were conducted to enhance our understanding of how the VIC model responds to changes.

The simulated groundwater recharge from the VIC model still presented an underestimation of over 80% in comparison to the averaged recharge observed globally in the AQUASTAT and Moeck datasets, but it also demonstrated its improvement in recharge estimation when compared to other hydrological models, such as PCR-GLOBWB. Therefore, our findings statistically agree to the results drawn by Berghuijs et al. (2022) that global-scale hydrological models underestimate groundwater recharge by half, particularly concerning the global averaged values.

When we adjusted the recharge input during sensitivity tests of the VIC model, the simulated groundwater flows followed the tendency more prominent in humid regions that the volume of flow increases with increased recharge, yet the volume drops as recharge declines. The simulated groundwater depths showed results differently from different recharge factors. There was no substantial difference about the depths between recharge factors of 1 and half, while the result from recharge factor of 2 revealed an unrealistic situation where depths approached 0 m across most regions globally, suggesting that water tables would be close to the land surface, and groundwater would flush almost every piece of land worldwide. Therefore, the result of the simulated depths from the recharge factor of 2 implicitly demonstrated that the findings from Berghuijs et al. (2022) using global average value to define the underestimation of global-scale hydrological models is less rigorous. Meanwhile, the empirical approach to estimating groundwater recharge is also inadequate to fully grasp the complexities of the groundwater system.

Through this study, we identified several deficiencies in our model that could be continuously improved, such as the considerations of human activities on recharge, calculations of percolation and capillary rise. For future studies, it is important to broaden our focus beyond the single parameter of recharge in the simulation process, and we also need to consider other influential factors in the groundwater system such as hydraulic conductivity, aquifer properties, etc. Lastly, future studies could prioritize regional recharge simulations over global ones to enhance the reliability of the hydrological models since there are more sufficient observational data at the regional scales.

References

Alley, W. M. (2009). Ground Water. In G. E. Likens (Ed.), *Encyclopedia of Inland Waters* (pp. 684–690). Academic Press. https://doi.org/10.1016/B978-012370626-3.00015-6

Al-Muqdadi, S.W.H., Khattab, M.O., & Abdulhussein, F.M. (2020). Groundwater flow-modeling and sensitivity analysis in a hyper arid region. *Water 12* (8). **https://doi.org/10.3390/w12082131**

Anderson, M. P., Woessner, W. W., & Hunt, R. J. (2015). Chapter 5—Spatial Discretization and Parameter Assignment. In M. P. Anderson, W. W. Woessner, & R. J. Hunt (Eds.), *Applied Groundwater Modeling (Second Edition)* (pp. 181–255). Academic Press. https://doi.org/10.1016/B978-0-08-091638-5.00005-5

Anderson, M. P., Woessner, W. W., & Hunt, R. J. (2015). Chapter 9 - Model Calibration: Assessing Performance. In M. P. Anderson, W. W. Woessner, & R. J. Hunt (Eds.), *Applied Groundwater Modeling (Second Edition)* (pp. 375–441). Academic Press. https://doi.org/10.1016/B978-0-08-091638-5.00009-2

Arnold, J. G., Muttiah, R. S., Srinivasan, R., & Allen, P. M. (2000). Regional estimation of base flow and groundwater recharge in the Upper Mississippi river basin. *Journal of Hydrology*, *227*(1), 21–40. https://doi.org/10.1016/S0022-1694(99)00139-0

Balek, J. (1988). Groundwater Recharge Concepts. Estimation of natural groundwater recharge. Springer, Dordrecht. doi:10.1007/978-94-015-7780-9_1

Barthel, R., Stangefelt, M., Giese, M., Nygren, M., Seftigen, K., & Chen, D. (2021). Current understanding of groundwater recharge and groundwater drought in Sweden compared to countries with similar geology and climate. *Geografiska Annaler: Series A, Physical Geography*, *103*(4), 323–345. https://doi.org/10.1080/04353676.2021.1969130

Berghuijs, W. R., Luijendijk, E., Moeck, C., Van Der Velde, Y., & Allen, S. T. (2022). Global Recharge Data Set Indicates Strengthened Groundwater Connection to Surface Fluxes. *Geophysical Research Letters*, *49*(23), e2022GL099010. https://doi.org/10.1029/2022GL099010

Boretti, A., & Rosa, L. (2019). Reassessing the projections of the World Water Development Report. *Npj Clean Water, 2*(1), Article 1. https://doi.org/10.1038/s41545-019-0039-9

Cassardo, C., & Jones, J. A. A. (2011). Managing Water in a Changing World. *Water*, *3*(2), Article 2. https://doi.org/10.3390/w3020618

Chilton, J. (1996). Groundwater. *Water Quality Assessments – A Guide to Use of Biota, Sediments and Water in Environmental Monitoring*, ed. Deborah Chapman (Cambridge: University Press), 412-14.

Combalicer, E. A., Lee, S. H., Ahn, S., Kim, D. Y., & Im, S. (2008). Comparing groundwater recharge and base flow in the Bukmoongol small-forested watershed, Korea. *Journal of Earth System Science*, *117*(5), 553–566. https://doi.org/10.1007/s12040-008-0052-8

Cuthbert, M. O., Taylor, R. G., Favreau, G., Todd, M. C., Shamsudduha, M., Villholth, K. G., et al. (2019). Observed controls on resilience of groundwater to climate variability in sub-Saharan Africa. *Nature, 572* (7768), 230–234. https://doi.org/10.1038/s41586-019-1441-7

Dash, S. S., Sahoo, B., & Raghuwanshi, N. S. (2021). How reliable are the evapotranspiration estimates by Soil and Water Assessment Tool (SWAT) and Variable Infiltration Capacity (VIC) models for catchment-scale drought assessment and irrigation planning? *Journal of Hydrology*, *592*, 125838. https://doi.org/10.1016/j.jhydrol.2020.125838

de Graaf, I. E. M., Sutanudjaja, E. H., Van Beek, L. P. H., & Bierkens, M. F. P. (2015). A high-resolution global-scale groundwater model. *Hydrology and Earth System Sciences*, *19*(2), 823–837. https://doi.org/10.5194/hess-19-823-2015

de Graaf, I. E. M., van Beek, R. L. P. H., Gleeson, T., Moosdorf, N., Schmitz, O., Sutanudjaja, E. H., & Bierkens, M. F. P. (2017). A global-scale two-layer transient groundwater model: Development and application to groundwater depletion. *Advances in Water Resources*, *102*, 53–67. https://doi.org/10.1016/j.advwatres.2017.01.011

de Graaf, I. E. M., Gleeson, T., (Rens) Van Beek, L. P. H., Sutanudjaja, E. H., & Bierkens, M. F. P. (2019). Environmental flow limits to global groundwater pumping. *Nature*, *574*(7776), 90–94. https://doi.org/10.1038/s41586-019-1594-4

Döll, P., Lehner, B., & Kaspar, F. (2002). Global Modeling of Groundwater Recharge. In Schmitz, G.H. (ed.): Proceedings of Third International Conference on Water Resources and the Environment Research, Technical University of Dresden, Germany, ISBN 3-934253-17-2

Döll, P., & Fiedler, K. (2008). Global-scale modeling of groundwater recharge. *Hydrology and Earth System Sciences*, *12*(3), 863–885. https://doi.org/10.5194/hess-12-863-2008

Droppers, B., Franssen, W. H. P., van Vliet, M. T. H., Nijssen, B., & Ludwig, F. (2020). Simulating human impacts on global water resources using VIC-5. *Geoscientific Model Development*, *13*(10), 5029–5052. https://doi.org/10.5194/gmd-13-5029-2020

EPA (United States Environmental Protection Agency). (2022). Climate change indicators: U.S. and global precipitation. Retrieved on March 16, 2024, from https://www.epa.gov/climate-indicators/climate-change-indicators-us-and-global-precipitation

Famiglietti, J. S. (2014). The global groundwater crisis. *Nature Climate Change*, *4*(11), 945–948. https://doi.org/10.1038/nclimate2425

FAO. (n.d.). AQUASTAT - FAO's Global Information System on Water and Agriculture: the birth of AQUASTAT. Retrieved February 13, 2024, from https://www.fao.org/aquastat/en/overview/history/

FAO. (n.d.). AQUASTAT - FAO's Global Information System on Water and Agriculture: irrigation by country. Retrieved on March 16, 2024, from https://www.fao.org/aquastat/en/geospatial-information/global-maps-irrigated-areas/irrigation-by-country

FAO. (2003). Chapter 2: Concepts and Definitions. Review of World Water Resources by Country. Rome: FAO. ISSN: 1020-1203.

FAO. (2003). Chapter 3: Methods used to compute water resources by country. Review of World Water Resources by Country. Rome: FAO. ISSN: 1020-1203.

FAO. (2005). *AQUSTAT online database, including water resources per country.* Retrieved October 24, 2023, from http://wwwfaoorg/nr/water/aquastat/indexstm.

FAO. (2019). *AQUASTAT Glossary.* Retrieved February 19, 2024, from https://www.fao.org/aquastat/en/databases/glossary/

Freyberg, J. v., Moeck, C., & Schirmer, M. (2015). Estimation of groundwater recharge and drought severity with varying model complexity. *Journal of Hydrology, 527*, 844-857. https://doi.org/10.1016/j.jhydrol.2015.05.025

Girvetz, E., Zganjar, C., Raber, G., Maurer, E., Kareiva, P., & Lawler, J. (2009). Applied Climate-Change Analysis: The Climate Wizard Tool. *PloS One*, *4*, e8320. https://doi.org/10.1371/journal.pone.0008320

Gou, J., Miao, C., Duan, Q., Tang, Q., Di, Z., Liao, W., Wu, J., & Zhou, R. (2020). Sensitivity Analysis-Based Automatic Parameter Calibration of the VIC Model for Streamflow Simulations Over China. *Water Resources Research*, *56*(1), e2019WR025968. https://doi.org/10.1029/2019WR025968

Government of Canada. (2013). *Water sources: groundwater.* Retrieved September 25, 2023, from https://www.canada.ca/en/environment-climate-change/services/water-overview/sources/groundwater.html

Grönwall, J., & Danert, K. (2020). Regarding Groundwater and Drinking Water Access through A Human Rights Lens: Self-Supply as A Norm. *Water*, *12*(2), Article 2. https://doi.org/10.3390/w12020419

Hamman, J. J., Nijssen, B., Bohn, T. J., Gergel, D. R., & Mao, Y. (2018). The Variable Infiltration Capacity model version 5 (VIC-5): Infrastructure improvements for new applications and reproducibility. *Geoscientific Model Development*, *11*(8), 3481–3496. https://doi.org/10.5194/gmd-11-3481-2018

Han, D., Currell, M. J., Cao, G., & Hall, B. (2017). Alterations to groundwater recharge due to anthropogenic landscape change. *Journal of Hydrology*, *554*, 545–557.

Hartmann, A. (2022). The Hydrology of Groundwater Systems—From Recharge to Discharge. In T. Mehner & K. Tockner (Eds.), *Encyclopedia of Inland Waters (Second Edition)*,*3*, 324–330. Elsevier. https://doi.org/10.1016/B978-0-12-819166-8.00097-9

Holmes, R.M., Shiklomanov, A.I., Suslove, A., Tretiakov, M., McClelland, J.W., Scott, L., Spencer, R.G.M., & Tank, S.E. (2021). River discharge. *NOAA Arctic*. DOI: 10.25923/zevf-ar65

Kummu, M., Guillaume, J. H. A., de Moel, H., Eisner, S., Flörke, M., Porkka, M., Siebert, S., Veldkamp, T. I. E., & Ward, P. J. (2016). The world's road to water scarcity: Shortage and stress in the 20th century and pathways towards sustainability. *Scientific Reports*, *6*, 38495. https://doi.org/10.1038/srep38495

Kundzewicz, Z. W., Krysanova, V., Benestad, R. E., Hov, Ø., Piniewski, M., & Otto, I. M. (2018). Uncertainty in climate change impacts on water resources. *Environmental Science & Policy*, *79*, 1–8. https://doi.org/10.1016/j.envsci.2017.10.008

Liang, X., Lettenmaier, D. P., Wood, E. F., & Burges, S. J. (1994). A simple hydrologically based model of land surface water and energy fluxes for general circulation models. *Journal of Geophysical Research: Atmospheres*, *99*(D7), 14415–14428. https://doi.org/10.1029/94JD00483

Liang, X., Xie, Z., & Huang, M. (2003). A new parameterization for surface and groundwater interactions and its impact on water budgets with the variable infiltration capacity (VIC) land surface model. *Journal of Geophysical Research: Atmospheres*, *108*(D16). https://doi.org/10.1029/2002JD003090

Li, B., Rodell, M., Peters-Lidard, C., Erlingis, J., Kumar, S., & Mocko, D. (2021). Groundwater Recharge Estimated by Land Surface Models: An Evaluation in the Conterminous United States. *Journal of Hydrometeorology*, *22*(2), 499–522. https://doi.org/10.1175/JHM-D-20-0130.1

Lin, Y-F., Wang, J., & Valocchi, A. J. (2008). Making groundwater recharge and discharge estimate maps in one day: An ArcGIS 9.2 application for water resources research. *ArcUser*, *11*(1), 32-35. https://www.esri.com/news/arcuser/0408/groundwater.html

Loudyi, D., Falconer, R., & Lin, B. (2014). *MODFLOW: An Insight Into Thirty Years Development Of A Standard Numerical Code For Groundwater Simulations*. 11th International Conference of Hydroinformatics, New York City, USA. https://academicworks.cuny.edu/cgi/viewcontent.cgi?article=1167&context=cc_conf_hic

MacDonald, A. M., Lark, R. M., Taylor, R. G., Abiye, T., Fallas, H. C., Favreau, G., Goni, I. B., Kebede, S., Scanlon, B., Sorensen, J. P. R., Tijani, M., Upton, K. A., & West, C. (2021). Mapping groundwater recharge in Africa from ground observations and implications for water security. *Environmental Research Letters*, *16*(3), 034012. https://doi.org/10.1088/1748-9326/abd661

Mahapatra, S., Jha, M. K., Biswal, S., & Senapati, D. (2020). Assessing Variability of Infiltration Characteristics and Reliability of Infiltration Models in a Tropical Sub-humid Region of India. *Scientific Reports*, *10*(1), Article 1. https://doi.org/10.1038/s41598-020-58333-8

Moeck, C., Grech-Cumbo, N., Podgorski, J., Bretzler, A., Gurdak, J. J., Berg, M., & Schirmer, M. (2020). A global-scale dataset of direct natural groundwater recharge rates: A review of variables, processes and relationships. *Science of The Total Environment*, *717*, 137042. https://doi.org/10.1016/j.scitotenv.2020.137042

Mohan, C., Western, A. W., Wei, Y., & Saft, M. (2018). Predicting groundwater recharge for varying land cover and climate conditions – a global meta-study. *Hydrology and Earth System Sciences*, *22*(5), 2689–2703. https://doi.org/10.5194/hess-22-2689-2018

Müller Schmied, H., Eisner, S., Franz, D., Wattenbach, M., Portmann, F. T., Flörke, M., & Döll, P. (2014). Sensitivity of simulated global-scale freshwater fluxes and storages to input data, hydrological model structure, human water use and calibration, *Hydrol. Earth Syst. Sci.*, *18*, 3511–3538, https://doi.org/10.5194/hess-18-3511-2014

Müller Schmied, H., Cáceres, D., Eisner, S., Flörke, M., Herbert, C., Niemann, C., Peiris, T. A., Popat, E., Portmann, F. T., Reinecke, R., Schumacher, M., Shadkam, S., Telteu, C.-E., Trautmann, T., & Döll, P. (2021). The global water resources and use model WaterGAP v2.2d: Model description and evaluation. *Geoscientific Model Development*, *14*(2), 1037–1079. https://doi.org/10.5194/gmd-14-1037-2021

Musie, W., & Gonfa, G. (2023). Fresh water resource, scarcity, water salinity challenges and possible remedies: A review. *Heliyon*, *9*(8), e18685. https://doi.org/10.1016/j.heliyon.2023.e18685

NASA Solar System Exploration. (2022). *In Depth | Earth*. (2022). Retrieved September 25, 2023, from https://solarsystem.nasa.gov/planets/earth/in-depth

Nan, Y., Bao-hui, M., & Chun-kun, L. (2011). Impact Analysis of Climate Change on Water Resources. *Procedia Engineering*, *24*, 643–648. https://doi.org/10.1016/j.proeng.2011.11.2710

Ojo, O. I., Otieno, F. A. O., & Ochieng, G. M. (2012). Groundwater: Characteristics, qualities, pollutions and treatments: An overview. *International Journal of Water Resources and Environmental Engineering*, *4*(6), 162–170. https://doi.org/10.5897/IJWREE12.038

Reinecke, R., Gnann, S., Stein, L., Bierkens, M., Graaf, I. de, Gleeson, T., OudeEssink, G., Sutanudjaja, E., Ruz-Vargas, C., Verkaik, J., & Wagener, T. (2023). *Global accessibility of groundwater remains highly uncertain*. https://eartharxiv.org/repository/view/5003/

Scanlon, B. R., Healy, R. W., & Cook, P. G. (2002). Choosing appropriate techniques for quantifying groundwater recharge. *Hydrogeology Journal*, *10*(1), 18–39. https://doi.org/10.1007/s10040-001-0176-2

Schilling, K. E., Langel, R. J., Wolter, C. F., & Arenas-Amado, A. (2021). Using baseflow to quantify diffuse groundwater recharge and drought at a regional scale. *Journal of Hydrology*, *602*, 126765. https://doi.org/10.1016/j.jhydrol.2021.126765

Sharp, J. (2010). The impacts of urbanization on groundwater systems and recharge. *Aqua Mundi*, *1*, 51–56. https://doi.org/10.4409/Am-004-10-0008

Sidabutar, N. V., Namara, I., Hartono, D. M., & Soesilo, T. E. B. (2017). The effect of anthropogenic activities to the decrease of water quality. *IOP Conference Series: Earth and Environmental Science*, *67*(1), 012034. https://doi.org/10.1088/1755-1315/67/1/012034

Sridhar, V., Billah, M. M., & Hildreth, J. W. (2018). Coupled Surface and Groundwater Hydrological Modeling in a Changing Climate. *Groundwater*, *56*(4), 618–635. https://doi.org/10.1111/gwat.12610

Stephens, G. L., Slingo, J. M., Rignot, E., Reager, J. T., Hakuba, M. Z., Durack, P. J., Worden, J., & Rocca, R. (2020). Earth's water reservoirs in a changing climate. *Proceedings. Mathematical, Physical, and Engineering Sciences*, *476*(2236), 20190458. https://doi.org/10.1098/rspa.2019.0458

Szilagyi, J., Zlotnik, V. A., & Jozsa, J. (2013). Net Recharge vs. Depth to Groundwater Relationship in the Platte River Valley of Nebraska, United States. *Groundwater*, *51*(6), 945–951. https://doi.org/10.1111/gwat.12007

Thai-Hoang, L., Thonga, T., Loce, H. T., Vane, P. T. T., Thuyf, P. T. P., & Thuoc, T. L. (2022). Influences of anthropogenic activities on water quality in the Saigon River, Ho Chi Minh City. *Journal of Water and Health, 20* (3). doi: 10.2166/wh.2022.233

The United Nations (U.N.). (n.d.). *Global issue: Population.* Retrieved October 24, 2023, from https://www.un.org/en/global-issues/population#:~:text=Our%20growing%20population&text=The%20world's%20population%20is%20expected,billion%20in%20the%20mid%2D2080s

Tzanakakis, V. A., Paranychianakis, N. V., & Angelakis, A. N. (2020). Water Supply and Water Scarcity. *Water*, *12*(9), Article 9. https://doi.org/10.3390/w12092347

Van Beek, L.P.H. & Bierkens, M.F.P. (2008). The Global Hydrological Model PCR-GLOBWB: Conceptualization, Parameterization and Verification. Report Department of Physical Geography, Utrecht University, Utrecht, The Netherlands, http://vanbeek.geo.uu.nl/suppinfo/vanbeekbierkens2009.pdf

Veeranna, J., & Jeet, P. (2020). Groundwater Recharges Technology for Water Resource Management: A Case Study. In B. Kalantar (Ed.), *Groundwater Management and Resources*. IntechOpen. https://doi.org/10.5772/intechopen.93946

Variable Infiltration Capacity (VIC) Macroscale Hydrological Model. (2021). *VIC model overview.* Retrieved February 19, 2024, from https://vic.readthedocs.io/en/master/Overview/ModelOverview/

Wang, G., Zhang, J., Xu, Y., Bao, Z., & Yang, X. (2017). Estimation of future water resources of Xiangjiang River Basin with VIC model under multiple climate scenarios. *Water Science and Engineering*, *10*(2), 87–96. https://doi.org/10.1016/j.wse.2017.06.003

Wardle, D. (2019). Groundwater as Hyperobject. *Mosaic: An Interdisciplinary Critical Journal*, *52*(2), 1–16. https://www.jstor.org/stable/26974155

Water Resources Mission Area. (2019). Artificial Groundwater Recharge. *U.S. Geological Survey*. Retrieved October 24, 2023, from https://www.usgs.gov/mission-areas/water-resources/science/artificial-groundwater-recharge#:~:text=Natural%20groundwater%20recharge%20occurs%20as,streams%2C%20lakes%2C%20and%20wetlands

Williams, M. (n.d.). *What percent of Earth is water?* Retrieved September 25, 2023, from https://phys.org/news/2014-12-percent-earth.html

Willis, T. M., & Black, A. S. (1996). Irrigation increases groundwater recharge in the Macquarie Valley. *Soil Research*, *34*(6), 837–847. https://doi.org/10.1071/sr9960837

Wood, E. F., Lettenmaier, D. P., & Zartarian, V. G. (1992). A land-surface hydrology parameterization with subgrid variability for general circulation models. *Journal of Geophysical Research: Atmospheres*, *97*(D3), 2717–2728. https://doi.org/10.1029/91JD01786

WRI (World Resources Institute): World Resources 2000–2001 –People and ecosystems: The fraying web of life, 2000.

WWAP (United Nations World Water Assessment Programme)/UN-Water. (2018). *The United Nations World Water Development Report 2018: Nature-Based Solutions for Water*. Paris, UNESCO. https://unesdoc.unesco.org/ark:/48223/pf0000261424

Zeydalinejad, N. (2022). Artificial neural networks vis-à-vis MODFLOW in the simulation of groundwater: A review. *Modeling Earth Systems and Environment*, *8*(3), 2911–2932. https://doi.org/10.1007/s40808-022-01365-y

Zomlot, Z., Verbeiren, B., Huysmans, M., & Batelaan, O. (2015). Spatial distribution of groundwater recharge and base flow: Assessment of controlling factors. *Journal of Hydrology: Regional Studies*, *4*, 349–368. https://doi.org/10.1016/j.ejrh.2015.07.005

Annexes

Annex 1. Coding notes when processing recharge data

```
time  Size:372    *** is unlimited ***
        standard_name: time
        units: days since 0001-01-01 00:00:00
        calendar: standard
        bounds: time_bnds
```

Figure A1.1. Time units displayed in the NetCDF file of the VIC simulated recharge in R.

```
#extract the data from netCDF file
tdata <- nc_open("/Users/mirandaxiao/Desktop/WUR/Thesis/R/Data/RQ 2/VIC-WUR_GWM_nat_GFDL-ESM4_historical_monthly_.1970-01_new.nc" )
print(tdata)

lon <- ncvar_get(tdata,"lon") #get longitude from the file
nlon <- dim(lon) #number of longitude, 720

lat <- ncvar_get(tdata,"lat") #get latitude from the file
nlat <- dim(lat) #number of latitude, 360

# Time section
time <- ncvar_get(tdata,"time") #extract time variable
tunits <- ncatt_get(tdata, "time", "units")
time_posix <- as.POSIXct("0001-01-01", tz="GMT",format = "%Y-%m-%d",origin = "1970-01-01") + time * 60 * 60 * 24 # Convert time values to days
# Only keep the month of each year and omit the days
time_month <- format(time_posix, "%Y-%m")
time_years <- format(time_posix, "%Y")
nt<-dim(time_posix) #number of months, 372

#extract groundwater recharge data from netCDF
recharge_array <- ncvar_get(tdata,"OUT_GWRECHARGE")
fillvalue <- ncatt_get (tdata, "OUT_GWRECHARGE", "_FillValue")
dim(recharge_array) #720, 360, 372
```

Figure A1.2. Key programming codes applied in R to organize the time units to monthly data of the VIC simulated recharge.

```
lonlat <- as.matrix(expand.grid(lon,lat)) #reshape longitude, latitude into a matrix
dim(lonlat) #259200, 2

m <- 1 #get a single slice of data
recharge_slice <- recharge_array[,,m]
recharge_vec <- as.vector(recharge_slice) #get the vector of recharge values
length(recharge_vec)

#create a datafrome to compute data into three columns, longitude, latitude, and recharge
recharge_df01 <- data.frame(cbind(lonlat,recharge_vec))
names(recharge_df01) <- c("lon","lat",paste("OUT_GWRECHARGE",as.character(m), sep="_")) #name of each column
#reshape data from array to vector
recharge_vec_long <- as.vector(recharge_array)
length(recharge_vec_long)
recharge_mat <- matrix(recharge_vec_long, nrow=nlon*nlat, ncol=nt) #matrix with 372 columns with monthly recharge only
dim(recharge_mat) #259200, 372
#create a data frame that combine longitude, latitude, and monthly recharge data
recharge_df02 <- data.frame(cbind(lonlat,recharge_mat))
names(recharge_df02) <- c("longitude", "latitude",time_month) #name of each column
dim(recharge_df02) # 259200,374
#Calculate the annual average values
num_columns <- ncol(recharge_df02) # There are 374 columns in this data frame,the first two columns are longitude and latitude
num_groups <- (num_columns - 2) %/% 12 # There are 31 groups, represent 31 years from 1970-2000
avg_matrix <- matrix(NA, nrow = nrow(recharge_df02), ncol = num_groups) # Calculate the average annual recharge in the data frame
for (i in 1:num_groups) {
  start_col <- 3 + (i - 1) * 12  # Adjusted index to start from the third column
  end_col <- start_col + 11
  avg_matrix[, i] <- rowMeans(recharge_df02[, start_col:end_col], na.rm = TRUE)
}
dim(avg_matrix) #259200,31
#create a data frame that combine longitude, latitude, and average annual recharge data
recharge_df03 <- data.frame(cbind(lonlat,avg_matrix))
names(recharge_df03) <- c("longitude", "latitude", "1970", "1971", "1972", "1973", "1974", "1975", "1976", "1977", "1978", "1979",
                          "1980", "1981", "1982", "1983", "1984", "1985", "1986", "1987", "1988", "1989", "1990", "1991", "1992", "1993",
                          "1994", "1995", "1996", "1997", "1998", "1999", "2000")
dim(recharge_df03) #259200,33
```

Figure A1.3. Key programming codes to reshape the rasterized VIC data to vector data and calculate the average recharge for every year in the period of 1970-2000.

```
#average recharge for each coordination in the period of 1970 to 2000
columns_overall_avg <- recharge_df03[, 3:ncol(recharge_df03)]
row_means <- rowMeans(columns_overall_avg, na.rm = TRUE)
recharge_df03$average <- row_means

#create a data frame that combine longitude, latitude, and periodically annual recharge data
recharge_df04 <- data.frame(cbind(lonlat,recharge_df03$average))
names(recharge_df04) <- c("longitude", "latitude","average_recharge") #name of each column
dim(recharge_df04) # 259200,3
```

Figure A1.4. Key programming codes to calculate the average groundwater recharge generated from the VIC model over the 31 years at each presented coordinate.

Annex 2. Supplementary information of the results (Chapter 3)

Table A2.1. Ranked countries of the observed groundwater recharge rates according to AQUASTAT

Country	GW recharge (mm/year)	Rank	Country	GW recharge (mm/year)	Rank
Costa Rica	730.1	1	Malaysia	195.21	45
Myanmar	684.45	2	Chile	190.49	46
Slovenia	663.7	3	France	188.47	47
Suriname	620.38	4	Democratic Republic of the Congo	181.05	48
Philippines	614.39	5	Laos	166.14	49
Comoros	609.57	6	Bahrain	165.76	50
Maldives	529.27	7	Malta	159.57	51
Ecuador	525.75	8	Guinea	155.6	52
Jamaica	496.7	9	Ireland	155.57	53
Nauru	489.06	10	Bangladesh	154.53	54
Guyana	487.79	11	USA	146.12	55
Liberia	471.8	12	Armenia	145.56	56
Nicaragua	458.2	13	Italy	142.67	57
Papua New Guinea	455.1	14	India	137.09	58
Colombia	449.17	15	Nepal	136.02	59
Mauritius	448.04	16	South Korea	135.29	60
Solomon Islands	442.77	17	Uruguay	129.08	61
Guinea-Bissau	426.99	18	Germany	127.81	62
Equatorial Guinea	374.74	19	Netherlands	120.35	63
Vanuatu	359.41	20	Uganda	119.91	64
Republic of Congo	353.72	21	Bolivia	119.61	65
Sierra Leone	349.09	22	Tobago	119.23	66
Honduras	347.25	23	Trinidad	119.23	67
Belize	337.74	24	Palestine	119.15	68
Lebanon	320.38	25	Ivory Coast	118.02	69
Guatemala	309.64	26	Sri Lanka	117.57	70
El Salvador	300.78	27	Ghana	110.23	71
Fiji	290.14	28	North Korea	106.21	72
Panama	281.9	29	Paraguay	104.1	73
Rwanda	277.19	30	Denmark	100.8	74
Burundi	276.23	31	Togo	100.15	75
Norway	251.92	32	Cambodia	97.22	76
Venezuela	248.71	33	Nigeria	95.87	77
Georgia	247.9	34	Madagascar	92.76	78
Indonesia	243.55	35	Central African Republic	90.62	79
Gabon	238.54	36	China	88.41	80
Peru	234.89	37	Estonia	87.27	81
Iceland	234.52	38	Turkey	86.9	82
Bhutan	230.94	39	Dominican Republic	85.94	83
Bosnia and Herzegovina	223.1	40	Thailand	81.43	84
Albania	219.07	41	Haiti	80.32	85
Vietnam	217.15	42	Nevis	79.43	86
Cameroon	215.44	43	Saint Kitts	79.43	87
Croatia	200.05	44	Greece	78.4	88

Table A2. 1. Continued

Country	GW recharge (mm/year)	Rank	Country	GW recharge (mm/year)	Rank
Belarus	76.61	89	Malawi	20.95	130
Mexico	76.58	90	Uzbekistan	19.65	131
Brazil	76.2	91	Czech Republic	18.17	132
Azerbaijan	75.43	92	Senegal	17.84	133
Latvia	72.77	93	Ethiopia	17.74	134
Japan	72.28	94	Brunei	17.6	135
Cyprus	71.47	95	Lithuania	16.94	136
Austria	71.45	96	Morocco	16.9	137
Kyrgyzstan	68.81	97	Lesotho	16.6	138
Hungary	64.36	98	Afghanistan	16.58	139
Pakistan	63	99	Mali	15.95	140
Zambia	62.5	100	Benin	15.51	141
Switzerland	60.28	101	Zimbabwe	15.41	142
Cuba	59.03	102	Kazakhstan	12.47	143
Spain	58.97	103	Tunisia	10.18	144
Timor-Leste	58.79	104	Australia	9.36	145
Bulgaria	56.73	105	Chad	9.08	146
Israel	55.83	106	Iraq	7.5	147
Gambia	47.64	107	Somalia	6.99	148
Angola	46.6	108	Finland	6.61	149
Russia	46.5	109	Jordan	6.08	150
Argentina	45.97	110	Kenya	5.97	151
Sweden	44.84	111	Qatar	5.21	152
Portugal	43.81	112	Oman	4.17	153
Tajikistan	42.19	113	Eritrea	4.08	154
UK	40.25	114	South Africa	3.94	155
Poland	39.86	115	Mongolia	3.9	156
Eswatini	38.6	116	Yemen	3.31	157
Canada	37.22	117	Botswana	2.94	158
Ukraine	36.72	118	Namibia	2.55	159
Moldova	36.14	119	Niger	2.11	160
Romania	35.79	120	United Arab Emirates	1.69	161
Slovakia	35.68	121	Egypt	1.5	162
Burkina Faso	34.82	122	Kuwait	1.15	163
Syria	33.2	123	Saudi Arabia	1.14	164
Cape Verde	32.16	124	Turkmenistan	0.86	165
Tanzania	31.87	125	Djibouti	0.69	166
Luxembourg	30.7	126	Algeria	0.66	167
Iran	30.38	127	Libya	0.37	168
Belgium	29.35	128	Mauritania	0.29	169
Mozambique	21.56	129			
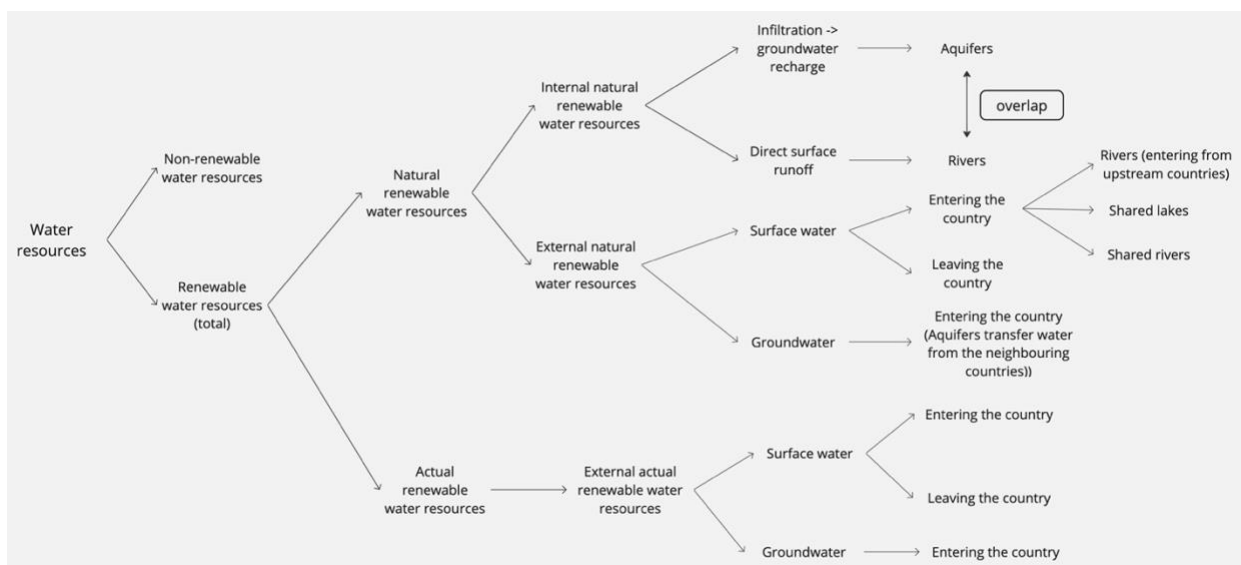
Figure A2.1. Relationships of various components in water resources according to AQUASTAT (FAO, 2003).
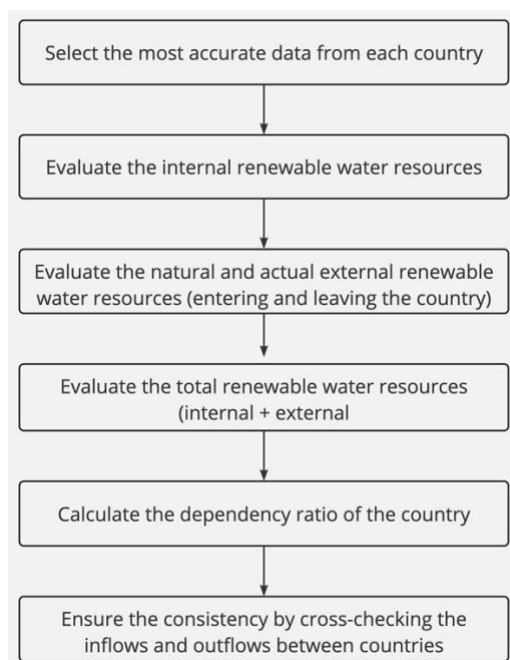
Figure A2.2. The six general steps applied by AQUASTAT in calculating different parts of the water system at the country scale (FAO, 2003).

Table A2. 2. Ranked countries of the simulated groundwater recharge rates according to the VIC model

Country	GW recharge (mm/year)	Rank	Country	GW recharge (mm/year)	Rank
Gabon	121.14	1	Madagascar	33.85	49
Maldives	116.84	2	Peru	33.41	50
Equatorial Guinea	114.85	3	Albania	32.66	51
Costa Rica	112.4	4	Guinea-Bissau	32.32	52
Papua New Guinea	97.82	5	Bosnia and Herzegovina	30.31	53
Panama	91.64	6	Sri Lanka	30.09	54
Brunei	90.92	7	Sweden	28.63	55
Colombia	87.54	8	Uruguay	27.35	56
Bangladesh	87.52	9	North Korea	26.73	57
Sierra Leone	84.45	10	Finland	24.82	58
Indonesia	81.08	11	Lebanon	24.15	59
Fiji	79.26	12	France	23.79	60
Liberia	77.92	13	Republic of Congo	23.39	61
Myanmar	77.52	14	USA	22.63	62
Iceland	76.71	15	Slovakia	21.9	63
Malaysia	75.35	16	Canada	21.54	64
Switzerland	73.29	17	Nigeria	21.48	65
Nepal	70.65	18	Bolivia	20.32	66
Nicaragua	64.89	19	Estonia	19.98	67
Solomon Islands	64.22	20	Vanuatu	19.65	68
Bhutan	62.88	21	Croatia	19.58	69
Guatemala	59.71	22	Latvia	19.41	70
Japan	58.14	23	Central African Republic	19.22	71
Ecuador	53.73	24	Timor-Leste	18.85	72
Vietnam	52.71	25	Mauritius	18.71	73
Norway	52.44	26	Jamaica	18.61	74
Cambodia	52.04	27	Netherlands	18.14	75
Belize	51.87	28	Ethiopia	18.05	76
Philippines	50.82	29	Belgium	17.64	77
Guyana	50.3	30	Denmark	17.28	78
Chile	49.23	31	Russia	16.3	79
Laos	49.19	32	Italy	15.87	80
Venezuela	46.89	33	Lithuania	15.78	81
Slovenia	46.5	34	Germany	15.41	82
South Korea	45.02	35	China	15.13	83
Georgia	44.81	36	Democratic Republic of the Congo	14.73	84
Ireland	44.78	37	Tobago	14.6	85
Suriname	44.1	38	Trinidad	14.6	86
Austria	39.12	39	Tajikistan	14.44	87
Honduras	38.28	40	Luxembourg	14.21	88
El Salvador	37.36	41	Belarus	14.18	89
Brazil	36.55	42	Dominican Republic	13.61	90
India	36.03	43	Ivory Coast	13.22	91
Guinea	35.81	44	Angola	13.04	92
UK	35.74	45	Mexico	12.99	93
Cameroon	34.68	46	Israel	12.81	94
Nauru	34.12	47	Poland	12.55	95
Thailand	34	48	Czech Republic	12.36	96

Table A2. 2. Continued

Country	GW recharge (mm/year)	Rank	Country	GW recharge (mm/year)	Rank
Portugal	11.79	97	Tanzania	6.46	134
Turkey	11.67	98	Ukraine	6.43	135
Eritrea	11.4	99	Cyprus	6.42	136
Zambia	11.37	100	Mauritania	6.4	137
Djibouti	11.18	101	Syria	6.36	138
Kyrgyzstan	11.12	102	Burundi	6.26	139
Romania	11.02	103	Somalia	5.97	140
Mozambique	10.87	104	Saudi Arabia	5.63	141
Malawi	10.67	105	Lesotho	5.59	142
Palestine	10.59	106	Gambia	5.43	143
Chad	10.41	107	Niger	5.33	144
Paraguay	10.05	108	Zimbabwe	5.14	145
Togo	9.58	109	Yemen	5.12	146
Haiti	9.57	110	Ghana	5.02	147
Benin	9.29	111	Moldova	5.02	148
Spain	8.81	112	Morocco	4.9	149
Cuba	8.59	113	Jordan	4.89	150
Rwanda	8.5	114	Kenya	4.84	151
Armenia	8.42	115	Cape Verde	4.8	152
Pakistan	8.13	116	Eswatini	4.74	153
Argentina	8.1	117	Uzbekistan	4.68	154
Uganda	8.09	118	Azerbaijan	4.5	155
Mali	7.87	119	Oman	4.37	156
Burkina Faso	7.81	120	Hungary	3.96	157
Kuwait	7.79	121	Turkmenistan	3.72	158
Tunisia	7.63	122	Botswana	3.41	159
Australia	7.58	123	Algeria	3.38	160
Iraq	7.57	124	Namibia	3.2	161
Senegal	7.57	125	Libya	3.15	162
Bulgaria	7.5	126	Kazakhstan	2.71	163
Malta	7.29	127	South Africa	2.71	164
Greece	7.23	128	Mongolia	2.06	165
Bahrain	7.18	129	Egypt	1.05	166
Afghanistan	7.08	130	Nevis	0.47	167
United Arab Emirates	6.92	131	Saint Kitts	0.47	168
Qatar	6.88	132	Comoros	0.32	169
Iran	6.84	133			
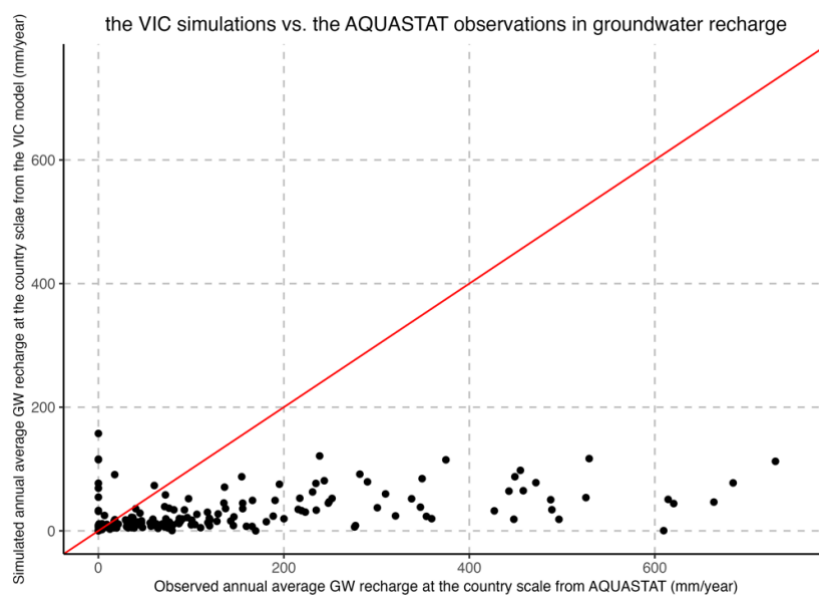
Figure A2.3. The scatter plot of the simulated VIC recharge and the observed AQUASTAT recharge at the country scale.
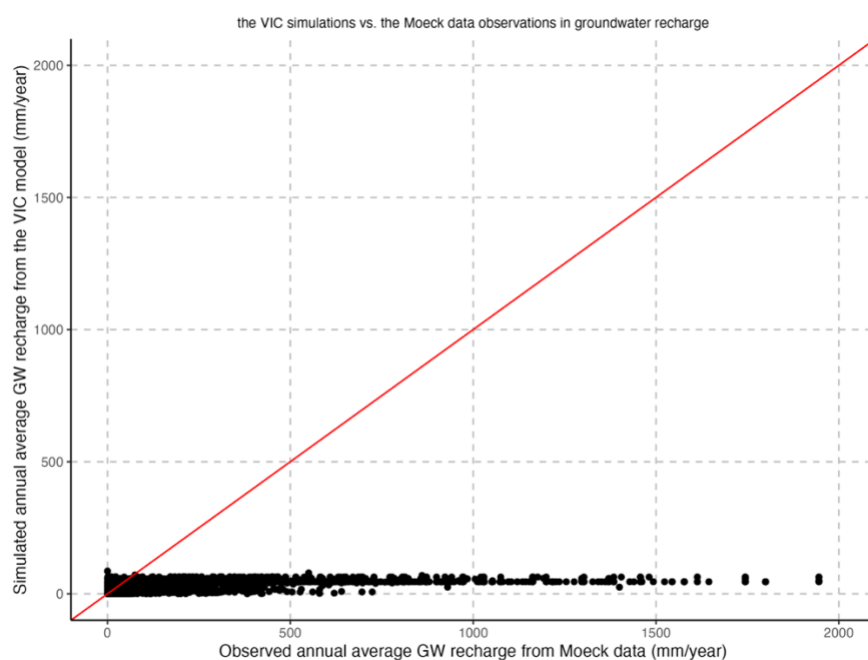
Figure A2.4. The scatter plot of the simulated VIC recharge and the observed Moeck recharge at the gridded scale.

Annex 3. Other supplementary information
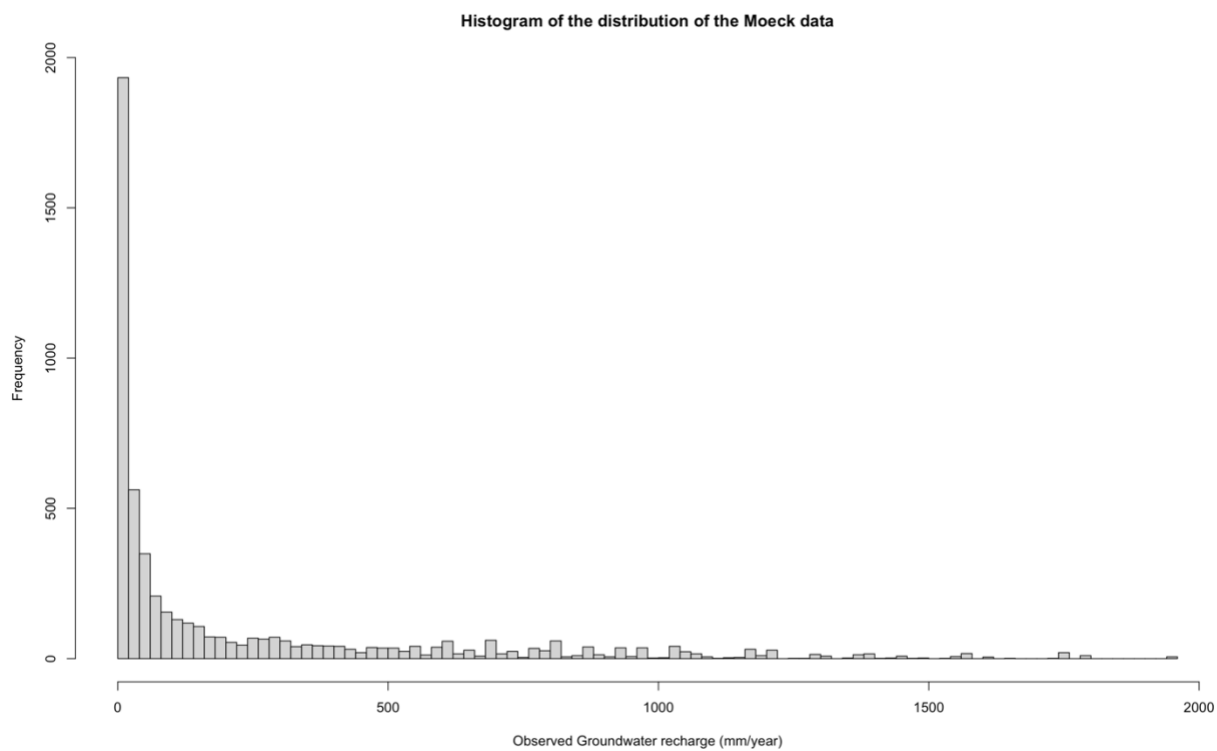
Figure A3.1. The histogram of the recharge data distribution from the Moeck observational dataset, with 20mm/year breaks (Moeck et al., 2020).